Analysis of the CH_3D Nonad from 2000 to 3300 cm^{-1}

A. Nikitin

Laboratory of Theoretical Spectroscopy, Institute of Atmospheric Optics, Russian Academy of Sciences, 634055 Tomsk, Russia

L.R. Brown

Jet Propulsion Laboratory, California Institute of Technology, 4800 Oak Grove Drive, Pasadena, CA 91109 USA

L. Féjard, J.P. Champion

Laboratoire de Physique (Unité associée au C.N.R.S.), Université de Bourgogne, 9 Avenue A. Savary, B.P. 47870 - 21078 Dijon, France

E-mail: Jean-Paul.Champion@u-bourgogne.fr

and

Vl. G. Tyuterev

Laboratoire de Spectroscopie Molculaire Atmosphriqu, (Unité associée au C.N.R.S.), Université de Reims, B.P. 1039 - 21078 Reims, France

As part of the simultaneous analysis of line positions and intensities of the first two polyads of monodeuterated methane, the results achieved for the 3 to 5 μm region are reported. It involves the three highest fundamentals, (ν_1, ν_2, ν_4) overlapped by overtone ($2\nu_3$, $2\nu_5$, $2\nu_6$) and combination ($\nu_3+\nu_6$, $\nu_3+\nu_5$, $\nu_5+\nu_6$) bands. The theoretical model was based on the global tensorial model implemented in the MIRS package (available on the web site http://www.u-bourgogne.fr/LPUB/MIRS.html). Some 10000 line positions and 2400 line intensities have been modeled to ± 0.00088 cm^{-1} and ± 3.6 % respectively, using measurements obtained at 0.0056 and 0.011 cm^{-1} resolution with the Fourier transform spectrometer at National Solar Observatory located at Kitt Peak. The strongest band in this polyad is $\nu_4(E)$ at 3016.7 cm^{-1} with a strength of $6.3 \times 10^{-18} cm^{-1}/(molecule\ cm^{-2})$ at 296 K; the weakest band is $2\nu_3(E)$ at 2597.7 cm^{-1} with a strength of 1.9×10^{-20} $cm^{-1}/(molecule\ cm^{-2})$ at 296 K. The total calculated absorption arising from the CH_3D nonad is 8.95×10^{-18} $cm^{-1}/(molecule\ cm^{-2})$ at 296 K.

Key Words: monodeuterated methane; CH_3D Nonad; infrared; fundamental bands; polyad; positions; intensities.

1. INTRODUCTION

The fact that monodeuterated methane (CH_3D) is a constituent trace species in the terrestrial and outer planet atmospheres (1) has motivated numerous high resolution investigations of its ro-vibrational spectra (2-33). Its ground state has been determined for both $^{12}CH_3D$ (3,4) and $^{13}CH_3D$ (5). Most infrared studies have been devoted to the bands within the triad region containing the three lowest fundamentals ν_6, ν_3 and ν_5 (3,5-10), while the region of the three highest fundamentals ν_2, ν_1 and ν_4 has received less attention (11-16). With a few exceptions (17-20), spectral intervals at shorter wavelengths are largely unexamined. Past studies of CH_3D also include line shape measurements for the lower triad and the $3\nu_2$ overtone (21-32).

The present authors previously reported the successful applications of an improved formalism (33) to the 12 vibrational states between the 900 - 3200 cm^{-1} (6,16). In the latter study (16), assignments given at 3.3 μm initially in 1972 by Olson (11) and at 4.8 μm by Chackerian et al. (13) were extended to all nine bands of the nonad. By treating all states simultaneously, 5208 positions of the nonad bands and 1007 nonad intensities were reproduced to $\pm$ 0.0047 cm^{-1} and $\pm$ 4.3%, respectively, and 2467 nonad−triad positions were fitted to $\pm$ 0.0043 cm^{-1}. However, identifications in the weaker bands were sparse, and there were numerous features left unassigned. To facilitate the assignment process, some 1000 selected line intensities were measured primarily in order to scale the predictions rather than to characterize the intensities of all the bands accurately. Finally, the standard deviation of the fit for line positions was an order of magnitude larger than the experimental precision.

Figure 1

An overview of the complexity of the task is given in Fig. 1 where the reduced upper state energy levels of the nonad states in cm^{-1} are plotted vs the upper state J. In our prior study, assignments were limited to less than $J = 19$ for the strong bands and $J = 13$ for the weak ones. For the present study of the nonad region, we obtained additional spectra at both low and high optical density in order to improve the accuracy of the strongest and weakest transitions. We measured an additional 1500 line intensities and assigned 5000 more transitions up to $J = 22$ for the strong bands and $J = 16$ for the weak ones. We further improved the modeling of the line positions and intensities to higher values of J so that the standard deviations of the fits more closely matched the measurement uncertainties.

2. EXPERIMENTAL DETAILS

The present results are based on a combination of prior data (16) and new data obtained primarily to improve the intensity analysis. Seven new scans were recorded at short paths (2.05 and 10.0 cm) in order to characterize the fundamental bands for the strongest lines, and two higher optical densities (at 150 cm path) were added for the weaker bands. A sample spectrum observed at 0.011 cm^{-1} resolution with the Fourier transform spectrometer located at Kitt Peak is plotted in Fig. 2 a and b, and the gas sample conditions of all the spectra used for intensities are shown in Table 1. The signal from a glowbar passed through absorption cells into the FTS, onto a CaF_2 beamsplitter and then was focused onto two matched InSb detectors. Pressures and temperatures were monitored continuously with calibrated capacitance gauges and thermistors, respectively, during the one hour integrations. Enriched samples (labelled as 98% and 99%) of the monodeurated methane were used. For a few scans, a second cell filled with CO was set in series with the CH_3D cell so that the lines in the $1-0$ band of CO (34) could be used to calibrate the nonad line positions. The spectra generally contained extra absorption arising from residual water and carbon dioxide at low pressure inside the inclosure of the FTS and also atmospheric absorption at 600 Torr from the intervals between the absorption cells, the source and detectors (see Fig. 2 a). The latter was purged using the effluent from a liquid nitrogen dewar.

Figure 2a - Figure 2b - Table 1

The measurements were retrieved from the laboratory spectra using curve-fitting techniques (35) illustrated in Fig. 3 . For this, each spectrum was measured individually by computing a synthetic spectrum and adjusting the assumed values of the positions, intensities and sometimes the self-broadened widths to reduce the differences between the observed and computed spectral digits. As mentioned previously, our prior effort (16) for intensities was aimed at determining the dominant transition moment of each band in order to extend the assignments. We were forced to use as input for the retrievals either a peak-finding linelist or approximate predictions. At the time we selected for measurement only known features and ignored many unidentified lines because they could not be included in the model. In the present study, however, we used an improved prediction (16) for the data reduction and were able to interpret many previously unidentified features. We particularly focused on improving the absolute accuracies for the fundamental transitions and the very weak bands. A more effective purging of the external path removed sufficiently more residual absorption from carbon dioxide so that CH_3D features between 2250 and 2400 cm^{-1} could be measured.

Figure 3 - Table 2

In Table 2, we give examples of the individual measurements of positions and intensities and corresponding averages (in bold). Each intensity is normalized for a gas sample that is 100% abundance of CH_3D, but no corrections have been made for the natural abundance of $^{12}CH_3D$ vs $^{13}CH_3D$ nor the observed 0.3% impurity of $^{12}CH_4$. The original temperature of the gas sample from which the measurement has been taken is shown, but each listed intensity is normalized to the corresponding value at 296 K; temperature uncertainty is 1.5 K for paths lengths greater than 11 cm, and 3 K for the three short cells (10.0, 5.00 and 2.05 cm). Typically, the measurements of the very strongest and the very weakest features involve only three or four scans while the intermediate intensity lines are determined using seven to eleven of the spectra. The rms is computed as (ith -average/average) to determine the agreement between individual spectra and the averaged value; this is taken as an indication of the experimental uncertainty. In general, there is good internal consistency from run to run for the intensities. Given the various sources of uncertainties (gas sample purity, path lengths and temperature), we estimate that the absolute accuracies of the intensities are 4% at best for

single lines, well-isolated from other features. Blended features and weaker transitions are thought to be good to 15%.

The absolute calibration of the line positions is derived from two spectra containing a second cell filled to observe the $1-0$ band of CO (34). Calibrated strong transitions of CH_3D were then transferred to the most of the other spectra; for the two highest optical density scans, many of the selected CH_3D lines were too saturated and so the calibration was checked using transitions of residual $^{12}CH_4$ (36). The precisions of the positions are $\pm$ 0.0003 cm^{-1} for well-isolated features. The absolute accuracies of transitions around 3000 cm^{-1} may be only 0.001 cm^{-1} because only one calibration standard at 2150 cm^{-1} was employed.

3. THEORETICAL MODEL

The theoretical framework of the present work is essentially the same as the one already described in our preliminary report (Ref. 16). Only basic or new features will be repeated or detailed here. The partially transformed ro-vibrational Hamiltonian adapted to the polyad structure of the CH_3D molecule is expressed as

$$\mathcal{H} = \mathcal{H}_{\{G.S.\}} + \mathcal{H}_{\{Triad\}} + \mathcal{H}_{\{Nonad\}} + \dots \quad (1)$$

where the subsequent terms correspond to successive polyads with increasing vibrational energies.

The effective Hamiltonians associated with the subsequent polyads include one, two or three sets of terms obtained by projection of the above equation onto the corresponding subspaces denoted by $< Polyad >$.

$$H^{<G.S.>} = H^{<G.S.>}_{\{G.S.\}} \quad (2)$$

$$H^{<Triad>} = H^{<Triad>}_{\{G.S.\}} + H^{<Triad>}_{\{Triad\}} \quad (3)$$

$$H^{<Nonad>} = H^{<Nonad>}_{\{G.S.\}} + H^{<Nonad>}_{\{Triad\}} + H^{<Nonad>}_{\{Nonad\}} . \quad (4)$$

In the present work, the parameters from $\mathcal{H}_{\{G.S.\}}$ involved in the effective Hamiltonians for the three polyads (ground state, triad and nonad) through the respective terms $H^{<G.S.>}_{\{G.S.\}}$, $H^{<Triad>}_{\{G.S.\}}$ and $H^{<Nonad>}_{\{G.S.\}}$, were kept fixed throughout the simultaneous analysis at the values reported recently by Ulenikov et al. (1999) (Ref. 4). The parameters from $H_{\{Triad\}}$ involved in both triad and nonad effective Hamiltonians through the terms $H^{<Triad>}_{\{Triad\}}$ and $H^{<Nonad>}_{\{Triad\}}$, were adjusted to fit simultaneously the "observed" energy levels recently published by Ulenikov et al. (2000) (Ref. 10) and the measured transition frequencies from both nonad and nonad−triad band systems.

The dipolar transition moment was similarly expressed in tensorial form. It is partially transformed according to the polyad pattern of the CH_3D molecule. In the present paper, only the nonad−G.S. system is considered, formally expressed as $M^{<GS,Nonad>}$ (16). The associated effective parameters were adjusted to fit the measurements of the nonad intensities extended in the present work. The results of the simultaneous analysis of the intensities of the triad and nonad−triad systems will be reported elsewhere.

Table 3a - Table 3b

In the present work, as in our preliminary analysis, all symmetry allowed terms from the Hamiltonian expansion up to the sixth order of approximation have been considered (1632 terms altogether). The last iteration of our simultaneous fit of positions yielded a unique set of 441 parameters (including 17 ground state parameters fixed and 424 statistically determined parameters). For brevity, only statistical informations are reported in Tables 3a and 3b of the present paper. For each vibrational type are quoted the total number of possible terms (symmetry allowed), the number of actually adjusted terms, the highest J dependence, and the matrix elements characteristics (ΔK_max and vibrational selection rules). In order to keep the number of adjusted parameters within reasonable bounds, the vibrationally off-diagonal terms have been selected in a

pragmatic way as already described in Refs. 6 and 16. Only the interaction terms between neighboring states have been released, whereas all interaction terms between non adjacent vibrational blocks were kept fixed to zero. A selection based on the reduction properties of effective Hamiltonians would certainly be preferable. However, this kind of theoretical investigation is very difficult for such a complex band system.

A complete parameter file including untruncated values (as input to the computer program) and the individual standard deviations is given in the Appendix. An electronic copy is also available on simple request from the authors and included into the computer package freely accessible from the web site http://www.u-bourgogne.fr/LPUB/MIRS.html. Among the 424 adjusted parameters, the number of vibrationally off-diagonal terms (227) is slightly larger than the number of vibrationally diagonal terms (197). It is worthwhile to emphasize that the ratios of the number of fitted data (or the number of bands) over the number of adjusted parameters were greatly minimized thanks to the global simultaneous treatment as compared with conventional band by band or even polyad by polyad treatments. As a matter of fact, in the present work, 424 parameters were adjusted on 11479 independent measurements, and the 441 effective Hamiltonian parameters involved, provided a description close to the experimental accuracy of the energy levels for 13 vibrational states (ground, triad and nonad) corresponding to 39 bands (6 fundamental, 3 overtone, 3 combination and 27 hot bands). Within this approach, on average, there are 27 data per adjusted parameter. Each vibrational state is described by less than 33 parameters and each vibrational band by less than 11 parameters.

For the effective transition moment of the nonad system all symmetry allowed terms up to J^2 dependent terms have been introduced (100 terms altogether). They correspond to expansions through the second order for fundamental bands and third order for overtone and combination bands. They account, in a systematic way, for various ro-vibrational effects usually described uncompletely by empirical Herman-Wallis type terms. The last iteration of the intensity fit yielded the set of 83 effective parameters listed in Table 4. The correspondence between the most basic terms and the parameters already considered in the literature are recalled in the last column. However, it should be emphasized that accurate predictions can only be obtained using the complete set of reported effective Hamiltonian and transition moment terms. The correlations between many of these terms would be rather difficult to describe and interpret. Although the number of statistically determined terms may seem relatively important with 83 adjusted parameters for 2459 measurements, the ratio of the number of fitted data over the number of adjusted parameters (about 29) is of the same order as for the fit of positions.

Table 4

4. RESULTS AND DISCUSSION

4.1. Position fit

Detailed statistics of the simultaneous fit of the positions of the triad, nonad and nonad−triad of CH_3D are given in Tables 5a, 5b and 6. The enhanced accuracy achieved in the present work arises from several improvements:

- The introduction of the new ground state constants recently determined by Ulenikov et al. (Ref. 4) allowed a better prediction of the higher J ground state energies and thus helped extending the assignment of weak features (forbidden and hot band transitions).
- The replacement of the former observed transition frequencies for the triad system (Tarrago et al. (1987) (Ref. 3)) by the "observed" energy levels reported recently by Ulenikov et al. (2000) (Ref. 10) allowed a more accurate description of the three lowest fundamental bands and, through our vibrational extrapolation approach, a more accurate modeling of the leading interactions among the upper states of the overtone and combination bands. As seen on Table 5a, the standard deviation on the fitted energies (0.00014 cm^{-1}) is

quite consistent with the results reported in Ref. 10, whereas the number of "triad" parameters (119 in the present work) is significantly smaller than in Ref. 10 (172 parameters). Furthermore, the maximum J dependence of the rovibrational terms is limited to J^6 in our model whereas several terms in J^7 , J^8 and higher are involved in the model of Ref. 10.

• Logically, as a consequence of the above improvements, the assignment process could be extended including weak lines from cold and hot bands, and to higher J values (up to $J = 23$). Numerous effective Hamiltonian parameters from the nonad part $H^{<Nonad>}_{\{Nonad\}}$ could then be interactively released while becoming statistically determined.

Table 5a - Table 5b - Table 6

Finally the standard deviations achieved for the nonad and nonad−triad systems were significantly improved: 0.00088 cm^{-1} and 0.00062 cm^{-1} to be compared to 0.0047 cm^{-1} and 0.0043 cm^{-1}, respectively, in our preliminary report (Ref. 16). As seen on Tables 5b and 6, the fitted positions cover all the nonad bands and most of the nonad−triad hot bands with a satisfactory uniformity in the level of precision, demonstrating the reliability of our model. Another probe of this can be seen in Table 5a from the standard deviations obtained, using the parameters of the present work, for the former triad observed transition (Ref. 3). The overall standard deviation (0.00051 cm^{-1}) is more than three times larger than the standard deviation on the new data. These values can be regarded as the upper limits of the experimental accuracies of the corresponding triad data sets.

4.2. Intensity fit

In our previous study, we used 12 purely vibrational transition moments and 18 J−dependent terms to model some 1000 line intensities up to $J = 16$. In the present effort, a total of 83 transitions moments are used (12 vibrational and 71 J−dependent) in order to model over 2400 intensities up to $J = 22$. Detailed statistics of the fit of the intensities of the nonad of CH_3D are given in the right hand side of Table 6. The results obtained for the triad and nonad−triad systems using the same Hamiltonian model and thus the same eigenvectors will be reported separately. As for the positions, the measurements covered all the bands of the nonad with a dynamical intensity range exceeding 4 orders of magnitude (Fig. 4). The selection of the data was done interactively as higher order parameters were released for the fit. A few measurements were rejected automatically on the basis of large discrepancies. In turn, a careful comparison of observed and synthetic spectra was achieved in order to confirm the experimental causes (like overlapping) for anomalous discrepancies. The model accuracy proved to be very similar for all the bands with an overall standard deviation of 3.6 % close to the experimental precision. In comparison with our preliminary study (Ref. 16) the number of fitted measurements was substantially increased while the standard deviation was slightly decreased. As for the positions, a larger number of statistically determined effective parameters could be obtained (Table 4).

Figure 4

The integrated intensities for the 13 components of the nonad are also shown in Table 6. These have been obtained by summing the line intensities greater than 10^{-25} cm/molecule at 296 K. The numbers of calculated lines are also indicated in the table.

The band strengths quoted in Table 6 are essentially governed by the purely vibrational transition moments ($R0(0,0A_1)$ type terms) given in Table 4. ν_4 is the strongest fundamental while ν_1 and ν_2 are an order of magnitude weaker. As expected, the combination bands are much weaker. Somewhat surprising, the transition moments of the overtones $2\nu_6$ and particularly $2\nu_5$ are rather large for both the A_1 and E components. However, the detailed results reflect the numerous interactions that give rise to complex intensity transfers. The most important is the Fermi interaction between ν_1 and $2\nu_5(A_1)$, whereas Coriolis and higher

order interactions also have a significant role. In the present work, the vibrational assignment is based on the eigenvector matrix. Due to the overall complexity of the nonad band system, this labeling may not always correspond to conventional methods based on line series. As a matter of fact, the major eigenvector component is smaller than $1/\sqrt{2}$ for 40% of the calculated energy levels at $J = 10$ and for 60% at $J = 20$. Finally, the importance of the fitted $J-$dependent terms in Table 4 should be emphasized. If set to zero and not adjusted, the standard deviation of the fitted intensities is drastically increased from 3.6% to 57%.

A line list of the predicted spectrum in three spectral intervals of the nonad (in ν_2, $\nu_3+\nu_5$ and ν_4) is reported in Tables 7a, 7b, 7c. The intensity threshold is 10^{-24} $cm/molecule$ at 296 K. A question mark in the assignment column indicates that $|\Delta K|$ exceeds 2 and points to perturbation allowed transitions. Note that the K assignment is done automatically by the computer program on the basis of the eigenvector component analysis. The residuals for positions and intensities are quoted when the corresponding data are included in the fits.

The corresponding synthetic spectrum is plotted in Figs. 5 a,b,c and compared with the experimental Kitt Peak spectrum recorded with pressures of 4.88 or 0.72 $Torr$ and a path length of 2.40 m. These portions include strong allowed and weak forbidden lines illustrating the ability of the theoretical model to account for all the observed features. In Fig. 5c one can see extra features in the experimental trace assigned to residual $^{12}CH_4$ lines.

Figure 5a - Figure 5b - Figure 5c

Remote sensing of monodeuterated methane in the terrestrial atmosphere has been hampered by incomplete spectroscopic information available in this spectral region. For example, atmospheric investigators (37,38) was able to use only five transitions of CH_3D in the analysis of the ATMOS spectra. Fortunately, the present study confirms exactly their assumed intensities reported by Rinsland et al. (38); the averaged ratio of prior (37,38) to the present intensities is 0.999 ± 0.025. Our new analysis now provides a much wider selection of well-characterized CH_3D transitions for atmospheric applications. These results, along with those from Fejard et al. (36), are available in the 2002 databases for HITRAN and GEISA (39,40).

5. CONCLUSION

After 30 years (11), the complex spectrum of CH_3D from 5 to 3 μm is well understood. All 13 components of the nine bands are assigned, and their positions and intensities are reproduced to within a factor of 2 of the experimental uncertainties. From the theoretical point a view, this work represents a first successful achievement of the tensorial model applied to a complex band system of symmetric top molecules involving both positions and intensities in a consistent way. It is a demonstrative example of the efficiency of the global approach of vibrational extrapolation. Future prospects to investigate bands of CH_3D at shorter wavelength are underway. Works are in progress using the MIRS package with a similar global approach to analyse the spectrum of CH_3Cl in the 3 μm region and at longer wavelength.

6. ACKNOWLEDGMENTS

We wish to thank M. Dulick and C. Plymate of the National Solar Observatory for their assistance in obtaining the CH_3D spectra using the FTS at Kitt Peak. Part of the research described in this paper was performed at the Jet Propulsion Laboratory, California Institute of Technology, under contract with The National Aeronautics and Space Administration. This work was also partly supported in the frame of the "Programme National de Plantologie" de l'Institut des Sciences de l'Univers (France).

7. REFERENCES

1. T. Encrenaz, Earth, Moon, and Planets 67, 77-87 (1995).

2. G. Tarrago, and M. Delaveau, J. Mol. Spectrosc. 119, 418-425 (1986).

3. G. Tarrago, M. Delaveau L. Fusina, and G. Guelachvili, J. Mol. Spectrosc. 126, 149-158 (1987).

4. O. N. Ulenikov, G. A. Onopenko, N. E. Tyabaeva, R. Anttila, S. Alanko, and J. Schroderus, J. Mol. Spectrosc. 193, 249-259 (1999).

5. O. N. Ulenikov, G. A. Onopenko, N. E. Tyabaeva, R. Anttila, S. Alanko, and J. Schroderus, J. Mol. Spectrosc. 201, 9-17 (2000).

6. A. Nikitin, J. P. Champion, Vl. G. Tyuterev, and L. R. Brown, J. Mol. Spectrosc. 184, 120-128 (1997).

7. R. J. Boyle, J. W. Halsey, and D. E. Jennings, J. Quant. Spectrosc. Rad. Transfer 33, 411-414 (1985).

8. G. Tarrago, G. Restelli, and F. Cappellani, J. Mol. Spectrosc. 129, 326-332 (1988).

9. P. Varanasi and S. Chudamani, J. Mol. Spectrosc. 134,440-444 (1989).

10. O. N. Ulenikov, G. A. Onopenko, N. E. Tyabaeva, R. Anttila, S. Alanko, and J. Schroderus, J. Mol. Spectrosc. 200, 1-15 (2000).

11. B. Olson, J. Mol. Spectrosc. 43, 190-xx (1972).

12. C. Chackerian Jr., E. S. Bus, W. B. Olson, and G. Guelachvili, J. Mol. Spectrosc. 117, 355-360 (1986).

13. C. Chackerian Jr., and G. Guelachvili, J. Mol. Spectrosc. 97, 316-332 (1983).

14. K. P. Carten, R. W. Lovejoy, and C. Chackerian Jr., J. Mol. Spectrosc. 159, 337-339 (1993).

15. C. B. Suarez, Spectrosc. Lett. 28, 429-439 (1995).

16. A. Nikitin, J. P. Champion, Vl. G. Tyuterev, L. R. Brown, G. Mellau, and M. Lock, J. Mol. Struct. 517-518, 1-24 (2000).

17. S. Carter, and J. M. Bowman, J. Phys. Chem. A 104, 2355-2361 (2000).

18. C. Boussin, B. L. Lutz, C. de Bergh, and A. Hamdouni, J. Quant. Spectrosc. Rad. Transfer 60, 501-514 (1998).

19. K. Deng, X. G. Wang, H. Lin, D. Wang, and Q. S. Zhu, Mol. Phys. 97, 787-795 (1999).

20. Z. Lin, K. Boraas, and J. P. Reilly, J. Mol. Spectrosc. 170, 266-278 (1995).

21. S. Chudamani and P. Varanasi, J. Quant. Spectrosc. Rad. Transfer 38, 179-181 (1987).

22. G. Blanquet, J. Walrand, and J. P. Bouanich, J. Mol. Spectrosc. 171, 525-532 (1995).

23. K. Jacquiez, M. Lepere, G. Blanquet, J. Walrand, and J. P. Bouanich, J. Mol. Spectrosc. 175, 386-389 (1996).

24. B. Lance, S. Ponsar, J. Walrand, M. Lepere, G. Blanquet, and J. P. Bouanich, J. Mol. Spectrosc. 189, 124-134 (1998).

25. C. Boussin, B. L. Lutz, A. Hamdouni, and C. de Bergh, J. Quant. Spectrosc. Rad. Transfer 63, 49-84 (1999).

26. V. Malathy Devi, D. C. Benner, M. A. H. Smith, C. P. Rinsland, and L. R. Brown, J. Mol. Struct. 517-518, 455-475 (2000).

27. Malathy Devi, D. C. Benner, M. A. H. Smith, and C. P. Rinsland, J. Quant. Spectrosc. Rad. Transfer 68, 135-161 (2001).

28. Malathy Devi, D. C. Benner, M. A. H. Smith, and C. P. Rinsland, J. Quant. Spectrosc. Rad. Transfer 68, 1-141 (2001).

29. J.J. Plateaux, L. Regalia, C. Boussin, and A. Barbe, J. Quant. Spectrosc. Rad. Transfer 68, 507-520 (2001).

30. V. Malathy Devi, D. C. Benner, M. A. H. Smith, C. P. Rinsland, and L. R. Brown, J. Quant. Spectrosc. Rad. Transfer 72, 139-191 (2002).

31. V. Malathy Devi, D. C. Benner, M. A. H. Smith, C. P. Rinsland, and L. R. Brown, J. Quant. Spectrosc. Rad. Transfer (in press).

32. V. Malathy Devi, D. C. Benner, M. A.H. Smith, C. P. Rinsland, and L. R. Brown, J. Quant. Spectrosc. Rad. Transfer (accepted).

33. A. Nikitin, J. P. Champion, and V. G. Tyuterev, J. Mol. Spectrosc. 182, 72-84 (1997).

34. A. G. Maki, and J. S. Wells, Wavenumber Calibration Tables from Heterodyne Frequency Measurements, NIST Special Publication 821 U.S. Government Printing Office (1991).

35. L. R. Brown, J. S. Margolis, R. H. Norton, and B. A. Stedry, Appl. Spectrosc. 37, 287-292 (1983).

36. L. Fejard, J. P. Champion, J. M. Jouvard, L. R. Brown, and A. S. Pine, J. Mol. Spectrosc. 201, 83-94 (2000).

37. F. W. Irion, E. J. Moyer, M. R. Gunson, C. P. Rinsland, Y. L Yung, H. A. Michelsen, R. J. Salawitch, A. Y. Chang, M. J. Newchurch, M. M. Abbas, M. C. Abrams, and R. Zander, Geophys. Res. Lett. 23, 2381-2384 (1996).

38 C. P. Rinsland, M. R. Gunson, J. C. Foster, R. A. Toth, C. B. Farmer, and R. Zander, J. Geophys. Res. Atmospheres 96, 1057-1068 (1991).

39. L. S. Rothman, C. P. Rinsland, A. Goldman, S. T. Massie, D. P. Edwards, J.-M. Flaud, A. Perrin, C. Camy-Peyret, V. Dana, J. Y-. Mandin, J. Schroeder, A. McCann, R. R. Gamache, R. B. Wattson, K. Yoshino, K. V. Chance, K. W. Jucks, L. R. Brown, V. Nemtchinov, and P. Varanasi, J. Quant. Spectrosc. Rad. Transfer 60, 665-710 (1998) and references therein.

40. N. Jacquinet-Husson, E. Arie, A. Barbe, L. R. Brown, C. Camy-Peyret, J. P. Champion, A. Chedin, A. Chursin, C. Clerbaux, G. Duxbury, J.-M. Flaud, N. Fourrie, A. Fayt, G. Graner, R. R. Gamache, A. Goldman, G. Guelachvili, J. M. Hartmann, J. C. Hillico, G. Lefevre, V. Naumenko, A. Nikitin, A. Perrin, D. Reuter, L. Rosenmann, L. S. Rothman, N. A. Scott, J. Selby, L. N. Sinitsa, J. M. Sirota, A. Smith, K. Smith,Vi. G. Tyuterev, R. H. Tipping, S. Urban, P. Varanasi, and M. Weber,, J. Quant. Spectrosc. Rad. Transfer 62, 205-254 (1999).

8. APPENDIX

9. FIGURE CAPTIONS

1. Reduced upper state energies in cm^{-1} versus upper state J for the nine bands (nonad) of CH_3D between 3 and 5 μm. The upper panel shows the calculated levels, and the lower panel shows the assigned levels.

2. The unapodized spectrum of CH_3D observed with the Fourier transform spectrometer located at Kitt Peak National Observatory. The resolution is 0.012 cm^{-1}.

a) The gas pressure is 15.5 $Torr$ at 293.4 K of an enriched sample containing 98%CH_3D. The optical path is 10 cm. The strongest band in the region is ν_4 near 3017 cm^{-1}. The band near 2350 cm^{-1} arises from residual CO_2.

b) The gas pressure is 20 $Torr$ at 295 K, and the path is 1.5 m. The strong Q branches near 2780 cm^{-1} belong to $\nu_3 + \nu_5(E)$.

3. Retrieval of positions and intensities by least squares curve fitting in the Q branch region of ν_4. The observed and synthetic spectra are overplotted in the lower panel and the residual differences are shown in the upper panel. The gas pressure is 4.98 $Torr$ at 296.1 K, and the optical path is 0.0205 cm.

4. Distribution of measured line intensities in the nonad. The observed intensities are plotted as a function of the line positions. Values in $cm^{-2}\ atm^{-1}$ at 296 K have been multiplied by 4.033×10^{-20} to convert to the intensity units of HITRAN ($cm/molecule$).

5. Examples of calculated (lower trace) and observed spectra of CH_3D in three spectral regions: a) $P(J = 14)$ branch of ν_2, b) $RQ(K = 0)$ of $\nu_3 + \nu_5$ (E) at 2780 cm^{-1} c) R branch of ν_4 at 3078 cm^{-1}... The gas pressure is 4.88 (a,b) or 0.72 (c) $Torr$ at 291 K, and the path is 2.4 m.

10. TABLE TITLES

1. Experimental conditions

2. Examples of retrieved positions and intensities for CH_3D

3a. Effective Hamiltonian for the ground state, triad and nonad of CH_3D Vibrationally diagonal terms

3b. Effective Hamiltonian for the ground state, triad and nonad of CH_3D Vibrationally off-diagonal terms

4. Effective transition moment terms for the nonad of CH_3D

5a. Detailed statistics of the simultaneous fit for the triad positions of CH_3D

5b. Detailed statistics of the simultaneous fit for the nonad - triad positions of CH_3D

6. Detailed statistics of the simultaneous fit for the nonad positions and intensities of CH_3D

7a. A sample of observed and calculated positions and intensities. $P(J = 14)$ branch of ν_2

7b. A sample of observed and calculated positions and intensities. $RQ(K = 0)$ of $\nu_3 + \nu_5$

7c. A sample of observed and calculated positions and intensities. R branch of ν_4

Table 1 - Experimental conditions

Pressure (Torr)	Path Length (m)	Temperature (K)	
1800 to 5500 cm^{-1} bandpass at 0.011 cm^{-1} resolution			
4.98	0.0205	296.1	n
6.60	0.0205	296.1	n
9.38	0.0205	296.1	n
4.88	0.05	291.0	
2.40	0.10	294.7	n
4.00	0.10	294.5	n
7.00	0.10	294.9	n
15.50	0.10	294.3	n
1.01	0.25	295.6	
2.00	0.25	295.6	
4.50	0.25	295.8	
9.73	0.25	295.9	
0.72	2.39	291.0	
4.88	2.39	291.0	
20.0	1.50	294.9	n
40.2	1.50	294.9	n
89.6	1.50	295.6	
1000 to 2650 cm^{-1} bandpass at 0.0056 cm^{-1} resolution			
0.13	25.0	296.4	
1.31	25.0	296.4	
1.31	97.0	296.4	

n indicates a new spectrum not available in Ref. 16.
The detectors are InSb and As-doped Si, respectively for the two spectral regions.

Table 2 - Examples of retrieved positions and intensities for CH_3D

Observed Position cm^{-1}	Obs-Av Diff cm^{-1}	Path Length m	Pressure Torr	Observed Intensity cm^{-2} atm^{-1}	Obs-Av Diff %	Temperature K
2160.768301	-0.00027	0.100	15.5	1.475×10^{-1}	-1.9	294.3
2160.768391	-0.00018	0.0205	6.60	1.410×10^{-1}	-6.2	296.1
2160.768407	-0.00016	0.250	2.00	1.555×10^{-1}	3.4	295.6
2160.768436	-0.00013	0.0205	9.38	1.600×10^{-1}	6.4	296.1
2160.768455	-0.00011	0.0205	4.98	1.432×10^{-1}	-4.7	296.1
2160.768586	0.00002	0.100	2.40	1.514×10^{-1}	0.7	294.7
2160.768631	0.00006	0.100	7.00	1.499×10^{-1}	-0.3	294.9
2160.768636	0.00007	0.100	4.00	1.556×10^{-1}	3.5	294.5
2160.768647	0.00008	0.250	1.01	1.534×10^{-1}	2.0	295.6
2160.768658	0.00009	0.250	4.50	1.478×10^{-1}	-1.7	295.8
2160.768754	0.00019	2.39	0.721	1.475×10^{-1}	-1.9	291.0
2160.768925	0.00036	0.050	4.88	1.513×10^{-1}	0.7	291.0
**2160.768569	0.00017	E"= 128.667	12	1.503×10^{-1}	3.4 = average	
2581.836560	-0.00046	1.50	40.2	2.447×10^{-3}	-1.9	294.9
2581.836870	-0.00015	1.50	20.0	2.420×10^{-3}	-3.0	294.9
2581.837332	0.00031	25.0	0.229	2.507×10^{-3}	0.5	296.4
2581.837333	0.00031	2.39	4.88	2.601×10^{-3}	4.3	291.0
**2581.837024	0.00033	E"= 23.279	4	2.494×10^{-3}	2.8 = average	
3080.060531	-0.00035	0.100	15.5	1.124×10^{-1}	1.6	294.3
3080.060643	-0.00023	0.0205	4.98	1.026×10^{-1}	-7.2	296.1
3080.060661	-0.00022	0.0205	9.38	1.142×10^{-1}	3.2	296.1
3080.060681	-0.00020	0.100	7.00	1.120×10^{-1}	1.2	294.9
3080.060687	-0.00019	0.0205	6.60	1.055×10^{-1}	-4.7	296.1
3080.060815	-0.00006	0.100	2.40	1.146×10^{-1}	3.5	294.7
3080.060816	-0.00006	0.100	4.00	1.143×10^{-1}	3.3	294.5
3080.060877	0.00000	0.250	2.00	1.132×10^{-1}	2.3	295.6
3080.061039	0.00016	0.250	4.50	1.107×10^{-1}	0.1	295.8
3080.061147	0.00027	0.250	1.01	1.094×10^{-1}	-1.1	295.6
3080.061742	0.00087	0.050	4.88	1.082×10^{-1}	-2.2	291.0
**3080.060876	0.00032	E"= 291.362	11	1.106×10^{-1}	3.3 = average	

Intensities are given at 296 K for 100% CH_3D

Table 3a - Effective Hamiltonian for the Ground State, Triad and Nonad of CH_3D
Vibrationally diagonal terms

Vib Type (degree)	Rot deg max	# of terms pos.	/ adj.	Matrix Elements Characteristics ΔK(max)	vibrational involvement	Lower order parameters / cm^{-1}
000000 000000 (0)	8	23	17	6	All vib diag blocks	$A_0 \simeq 5.25$ $B_0 \simeq 3.88$
001000 001000 (2)	6	14	11	6	$\nu_3, 2\nu_3, \nu_3+\nu_5, \nu_3+\nu_6$	$\sigma_3 \simeq 1307$
000010 000010 (2)	6	39	25	6	$\nu_5, 2\nu_5, \nu_3+\nu_5, \nu_5+\nu_6$	$\sigma_5 \simeq 1472$
000001 000001 (2)	6	39	21	5	$\nu_6, 2\nu_6, \nu_3+\nu_6, \nu_5+\nu_6$	$\sigma_6 \simeq 1161$
100000 100000 (2)	6	14	9	6	ν_1	$\sigma_1 \simeq 2969$
010000 010000 (2)	6	14	9	6	ν_2	$\sigma_2 \simeq 2200$
000100 000100 (2)	6	39	21	5	ν_4	$\sigma_4 \simeq 3017$
002000 002000 (4)	4	7	5	3	$2\nu_3$	$\Delta\sigma_{33} \simeq -15$
000020 000020 (4)	4	36	24	4	$2\nu_5$	$\Delta\sigma^0_{55} \simeq -34$ $\Delta\sigma^2_{55} \simeq -5.6$
000002 000002 (4)	4	36	22	3	$2\nu_6$	$\Delta\sigma^0_{66} \simeq -5.9$ $\Delta\sigma^2_{66} \simeq 1.5$
001010 001010 (4)	4	18	13	4	$\nu_3+\nu_5$	$\Delta\sigma_{35} \simeq -3.7$
001001 001001 (4)	4	18	13	4	$\nu_3+\nu_6$	$\Delta\sigma_{36} \simeq -3.4$
000011 000011 (4)	4	59	24	3	$\nu_5+\nu_6$	$\Delta\sigma^{A_1}_{56} \simeq -9.3$ $\Delta\sigma^{A_2}_{56} \simeq 10.2$ $\Delta\sigma^{E}_{56} \simeq -1.8$
Total		356	214		*(197 adjsuted parameters)*	

Table 3b - Effective Hamiltonian for the Ground State, Triad and Nonad of CH_3D
Vibrationally off-diagonal terms

Vib Type (degree)	Rot deg max	Vibrational Selection Rules	# of terms pos.	/ adj.	ΔK(max)
001000 000010 (2)	6	$\nu_3 \leftrightarrow \nu_5, 2\nu_3 \leftrightarrow \nu_3+\nu_5$ $2\nu_5 \leftrightarrow \nu_3+\nu_5,\ \nu_3+\nu_6 \leftrightarrow \nu_5+\nu_6$	27	17	5
001000 000001 (2)	6	$\nu_3 \leftrightarrow \nu_6, 2\nu_3 \leftrightarrow \nu_3+\nu_6$ $2\nu_6 \leftrightarrow \nu_3+\nu_6,\ \nu_3+\nu_5 \leftrightarrow \nu_5+\nu_6$	27	12	5
000010 000001 (2)	6	$\nu_5 \leftrightarrow \nu_6, 2\nu_5 \leftrightarrow \nu_5+\nu_6$ $2\nu_6 \leftrightarrow \nu_5+\nu_6,\ \nu_3+\nu_5 \leftrightarrow \nu_3+\nu_6$	57	33	5
100000 010000 (2)	6	$\nu_1 \leftrightarrow \nu_2$	17	0	-
100000 000100 (2)	6	$\nu_1 \leftrightarrow \nu_4$	27	21	5
010000 000100 (2)	6	$\nu_2 \leftrightarrow \nu_4$	27	0	-
100000 002000 (3)	5	$\nu_1 \leftrightarrow 2\nu_3$	10	0	-
100000 000020 (3)	5	$\nu_1 \leftrightarrow 2\nu_5$	28	10	4
100000 000002 (3)	5	$\nu_1 \leftrightarrow 2\nu_6$	28	0	-
100000 001010 (3)	5	$\nu_1 \leftrightarrow \nu_3+\nu_5$	18	9	2
100000 001001 (3)	5	$\nu_1 \leftrightarrow \nu_3+\nu_6$	18	0	-
100000 000011 (3)	5	$\nu_1 \leftrightarrow \nu_5+\nu_6$	38	0	-
010000 002000 (3)	5	$\nu_2 \leftrightarrow 2\nu_3$	10	0	-
010000 000020 (3)	5	$\nu_2 \leftrightarrow 2\nu_5$	28	0	-
010000 000002 (3)	5	$\nu_2 \leftrightarrow 2\nu_6$	28	11	4
010000 001010 (3)	5	$\nu_2 \leftrightarrow \nu_3+\nu_5$	18	0	-
010000 001001 (3)	5	$\nu_2 \leftrightarrow \nu_3+\nu_6$	18	0	-
010000 000011 (3)	5	$\nu_2 \leftrightarrow \nu_5+\nu_6$	38	0	-
000100 002000 (3)	5	$\nu_4 \leftrightarrow 2\nu_3$	18	0	-
000100 000020 (3)	5	$\nu_4 \leftrightarrow 2\nu_5$	56	23	4
000100 000002 (3)	5	$\nu_4 \leftrightarrow 2\nu_6$	56	0	-
000100 001010 (3)	5	$\nu_4 \leftrightarrow \nu_3+\nu_5$	38	17	5
000100 001001 (3)	5	$\nu_4 \leftrightarrow \nu_3+\nu_6$	38	0	-
000100 000011 (3)	5	$\nu_4 \leftrightarrow \nu_5+\nu_6$	74	0	-
002000 000020 (4)	4	$2\nu_3 \leftrightarrow 2\nu_5$	19	0	-
002000 000002 (4)	4	$2\nu_3 \leftrightarrow 2\nu_6$	19	0	-
002000 001010 (4)	4	$2\nu_3 \leftrightarrow \nu_3+\nu_5$	11	0	-
002000 001001 (4)	4	$2\nu_3 \leftrightarrow \nu_3+\nu_6$	11	4	2
002000 000011 (4)	4	$2\nu_3 \leftrightarrow \nu_5+\nu_6$	24	11	3
000020 000002 (4)	4	$2\nu_5 \leftrightarrow 2\nu_6$	54	0	-
000020 001010 (4)	4	$2\nu_5 \leftrightarrow \nu_3+\nu_5$	35	0	-
000020 001001 (4)	4	$2\nu_5 \leftrightarrow \nu_3+\nu_6$	35	0	-
000020 000011 (4)	4	$2\nu_5 \leftrightarrow \nu_5+\nu_6$	70	0	-
000002 001010 (4)	4	$2\nu_6 \leftrightarrow \nu_3+\nu_5$	35	0	-
000002 001001 (4)	4	$2\nu_6 \leftrightarrow \nu_3+\nu_6$	35	13	3
000002 000011 (4)	4	$2\nu_6 \leftrightarrow \nu_5+\nu_6$	70	0	-
001010 001001 (4)	4	$\nu_3+\nu_5 \leftrightarrow \nu_3+\nu_6$	24	0	-
001010 000011 (4)	4	$\nu_3+\nu_5 \leftrightarrow \nu_5+\nu_6$	46	17	3
001001 000011 (4)	4	$\nu_3+\nu_6 \leftrightarrow \nu_5+\nu_6$	46	18	3
Total			1276	227	

Table 4 - Effective Transition Moment Terms for the Nonad of CH_3D

	Tensorial Nomenclature		Parameter value		Nomenclature
	Rotational	Vibrational	Computer Input	Rounded (St. Dev.)	Ref. (8)
			Fundamental Bands		
1	R0(0,0A$_1$)	000000 100000	0.77261065607E-02	7.763(21) 10^{-3}	$1/(3\sqrt{2})d_1$
2	R1(1,1E)	000000 100000	0.19161846373E-03	1.925(14) 10^{-4}	$d_1^{(1)}$
3	R2(0,0A$_1$)	000000 100000	-0.35751824074E-06	-3.59(92) 10^{-7}	
4	R2(2,0A$_1$)	000000 100000	-0.75053947440E-06	-7.54(97) 10^{-7}	
5	R2(2,1E)	000000 100000	-0.13089350863E-05	-1.31(10) 10^{-6}	
6	R0(0,0A$_1$)	000000 010000	0.96727778135E-02	9.714(20) 10^{-3}	$1/(3\sqrt{2})d_2$
7	R1(1,1E)	000000 010000	0.64228687801E-04	6.45(12) 10^{-5}	$d_2^{(1)}$
8	R2(0,0A$_1$)	000000 010000	-0.50374952106E-06	-5.28(58) 10^{-7}	
9	R0(0,0A$_1$)	000000 000100	-0.47797707883E-01	-4.802(10) 10^{-2}	$2/3d_4$
10	R1(1,1E)	000000 000100	-0.37067725936E-04	-3.72(18) 10^{-5}	$d_4^{(1)}$; $d_4^{(2)}$; $d_4^{(6)}$
11	R1(1,0A$_2$)	000000 000100	-0.99027901881E-04	-9.95(39) 10^{-5}	$d_4^{(1)}$; $d_4^{(2)}$; $d_4^{(6)}$
12	R1(1,1E)	000000 000100	0.30760172566E-03	3.092(80) 10^{-4}	$d_4^{(1)}$; $d_4^{(2)}$; $d_4^{(6)}$
13	R2(0,0A$_1$)	000000 000100	0.11423696906E-05	1.14(28) 10^{-6}	
14	R2(2,0A$_1$)	000000 000100	-0.10939814661E-05	-1.09(23) 10^{-6}	
15	R2(2,1E)	000000 000100	-0.30536258283E-05	-3.07(50) 10^{-6}	
			Combination Bands		
16	R0(0,0A$_1$)	000000 001010	0.36882866609E-02	3.7069(96) 10^{-3}	
17	R1(1,1E)	000000 001010	0.18945484952E-05	1.91(55) 10^{-6}	
18	R1(1,0A$_2$)	000000 001010	-0.23574914579E-04	-2.368(95) 10^{-5}	
19	R1(1,1E)	000000 001010	-0.48362376275E-04	-4.84(27) 10^{-5}	
20	R2(2,1E)	000000 001010	-0.57444354289E-06	-5.76(51) 10^{-7}	
21	R2(2,2E)	000000 001010	-0.32084057420E-06	-3.29(79) 10^{-7}	
22	R2(0,0A$_1$)	000000 001010	0.53368376940E-06	5.42(60) 10^{-7}	
23	R2(2,0A$_1$)	000000 001010	0.65215423270E-06	6.57(54) 10^{-7}	
24	R0(0,0A$_1$)	000000 001001	0.13756691084E-02	1.3818(43) 10^{-3}	
25	R1(1,1E)	000000 001001	0.16311439608E-04	1.635(28) 10^{-5}	
26	R1(1,0A$_2$)	000000 001001	-0.21007860501E-04	-2.103(31) 10^{-5}	
27	R1(1,1E)	000000 001001	-0.70888640852E-05	-7.12(56) 10^{-6}	
28	R2(2,1E)	000000 001001	0.48999803675E-06	4.95(21) 10^{-7}	
29	R2(2,2E)	000000 001001	-0.17385867659E-06	-1.72(32) 10^{-7}	
30	R2(0,0A$_1$)	000000 001001	-0.60030946731E-06	-6.14(27) 10^{-7}	
31	R2(2,0A$_1$)	000000 001001	-0.29634292876E-06	-3.08(23) 10^{-7}	
32	R2(2,1E)	000000 001001	0.14972683315E-06	1.47(36) 10^{-7}	
33	R2(2,2E)	000000 001001	0.42843476729E-06	4.23(27) 10^{-7}	
34	R0(0,0A$_1$)	000000 000011	0.15925647096E-02	1.6002(31) 10^{-3}	
35	R0(0,0A$_1$)	000000 000011	-0.76795728083E-03	-7.717(26) 10^{-4}	
36	R1(1,0A$_2$)	000000 000011	-0.51823063669E-04	-5.209(26) 10^{-5}	
37	R1(1,1E)	000000 000011	-0.53852640069E-04	-5.413(21) 10^{-5}	
38	R1(1,1E)	000000 000011	0.43047675252E-04	4.328(28) 10^{-5}	
39	R1(1,1E)	000000 000011	-0.54557207284E-04	-5.481(24) 10^{-5}	
40	R1(1,0A$_2$)	000000 000011	0.48151200102E-04	4.835(40) 10^{-5}	
41	R1(1,1E)	000000 000011	0.15927174102E-04	1.601(30) 10^{-5}	
42	R2(0,0A$_1$)	000000 000011	0.38043861603E-06	3.82(17) 10^{-7}	
43	R2(2,0A$_1$)	000000 000011	-0.84679199038E-07	-8.5(17) 10^{-8}	
44	R2(2,1E)	000000 000011	0.22681980513E-06	2.27(21) 10^{-7}	
45	R2(2,2E)	000000 000011	0.33664172999E-06	3.38(14) 10^{-7}	
46	R2(2,2E)	000000 000011	-0.66998657584E-06	-6.66(32) 10^{-7}	
47	R2(2,0A$_1$)	000000 000011	-0.55355216259E-06	-5.57(31) 10^{-7}	
48	R2(2,1E)	000000 000011	0.62578056627E-06	6.30(36) 10^{-7}	
49	R2(2,2E)	000000 000011	-0.23180507171E-06	-2.33(18) 10^{-7}	

Table 4 - Effective Dipole Moment Terms for the Nonad of CH_3D (Continued)

	Nomenclature		Parameter value	
	Rotational	Vibrational	Computer Input	Rounded (St. Dev.)
		Overtone Bands		
50	R0(0,0A$_1$)	000000 002000	0.17864839147E-02	1.7952(34) 10^{-3}
51	R1(1,1E)	000000 002000	0.53172609357E-04	5.346(31) 10^{-5}
52	R2(0,0A$_1$)	000000 002000	0.27876453805E-06	2.80(17) 10^{-7}
53	R2(2,0A$_1$)	000000 002000	0.94534009221E-07	9.5(15) 10^{-8}
54	R2(2,1E)	000000 002000	-0.82854268560E-06	-8.33(18) 10^{-7}
55	R2(2,2E)	000000 002000	-0.40674252612E-06	-4.06(86) 10^{-7}
56	R0(0,0A$_1$)	000000 000020	-0.60428104866E-02	-6.072(18) 10^{-3}
57	R0(0,0A$_1$)	000000 000020	0.78530870450E-02	7.891(17) 10^{-3}
58	R1(1,1E)	000000 000020	0.18135509519E-04	1.82(12) 10^{-5}
59	R1(1,0A$_2$)	000000 000020	-0.24607539343E-04	-2.47(19) 10^{-5}
60	R1(1,1E)	000000 000020	-0.80343893606E-04	-8.06(20) 10^{-5}
61	R1(1,1E)	000000 000020	-0.36093343513E-04	-3.62(12) 10^{-5}
62	R2(2,2E)	000000 000020	0.10892821576E-05	1.093(94) 10^{-6}
63	R2(0,0A$_1$)	000000 000020	0.68710848627E-06	6.88(80) 10^{-7}
64	R2(2,0A$_1$)	000000 000020	-0.66339809265E-06	-6.66(84) 10^{-7}
65	R2(2,1E)	000000 000020	-0.19956643554E-05	-2.00(20) 10^{-6}
66	R2(2,2E)	000000 000020	0.37502365247E-05	3.77(13) 10^{-6}
67	R2(2,1E)	000000 000020	-0.38606822899E-06	-3.9(10) 10^{-7}
68	R2(2,2E)	000000 000020	0.14772432238E-05	1.48(22) 10^{-6}
69	R0(0,0A$_1$)	000000 000002	-0.44137752132E-02	-4.436(10) 10^{-3}
70	R0(0,0A$_1$)	000000 000002	-0.46775239911E-02	-4.700(13) 10^{-3}
71	R1(1,1E)	000000 000002	0.31216975449E-04	3.141(33) 10^{-5}
72	R1(1,0A$_2$)	000000 000002	-0.35004799084E-04	-3.517(56) 10^{-5}
73	R1(1,1E)	000000 000002	0.13880582342E-04	1.25(12) 10^{-5}
74	R1(1,1E)	000000 000002	-0.18298871681E-04	-1.871(47) 10^{-5}
75	R2(2,1E)	000000 000002	0.56777624564E-06	5.72(31) 10^{-7}
76	R2(2,2E)	000000 000002	0.10209869044E-05	1.067(34) 10^{-6}
77	R2(0,0A$_1$)	000000 000002	-0.12866065304E-05	-1.282(54) 10^{-6}
78	R2(2,0A$_1$)	000000 000002	0.15836412724E-05	1.595(72) 10^{-6}
79	R2(0,0A$_1$)	000000 000002	-0.41772453820E-06	-4.18(47) 10^{-7}
80	R2(2,1E)	000000 000002	0.17643363055E-05	1.93(14) 10^{-6}
81	R2(2,2E)	000000 000002	0.15987259248E-05	1.613(50) 10^{-6}
82	R2(2,1E)	000000 000002	-0.27837014033E-05	-2.78(11) 10^{-6}
83	R2(2,2E)	000000 000002	0.62370293381E-06	6.38(28) 10^{-7}

For clarity, only a simplified nomenclature is reported here. The complete unambiguous tensorial nomenclature is available from the electronic file at http://www.u-bourgogne.fr/LPUB/MIRS.html

Table 5a - Detailed Statistics of the Simultaneous Fit of the Triad, Nonad and Nonad–Triad of CH_3D Triad system

Band	Origin cm^{-1}	Nb Fitted Energies (a)	Jmax	St. Dev. 10^{-3} cm^{-1}	Nb Obs Positions (b)	St. Dev. 10^{-3} cm^{-1}
$\nu_6(E)$	1161.103	595	24	0.15	1745	0.53
$\nu_3(A_1)$	1306.848	292	23	0.13	818	0.50
$\nu_5(E)$	1472.023	492	21	0.17	1421	0.43
Triad (Present work)		1379	24	0.14	3467	0.51
Triad (Ref. 16)					3467	2.1

(a) Observed Energy levels reported by Ulenikov et al. (10)
(b) Assignments Reported by Tarrago et al. (3)

Table 5b - Detailed Statistics of the Simultaneous Fit of the Triad, Nonad and Nonad−Triad of CH_3D Hot Band System

Band	Origin cm^{-1}	Nb Fitted Positions	Jmax	St. Dev. 10^{-3} cm^{-1}
$2\nu_6(E) - \nu_5$	851	0	-	-
$\nu_3 + \nu_6 - \nu_5$	993	0	-	-
$2\nu_6(A_1) - \nu_3$	1010	0	-	-
$2\nu_6(E) - \nu_3$	1016	1	14	-
$\nu_2 - \nu_6$	1039	7	13	0.30
$2\nu_3 - \nu_5$	1126	8	19	1.00
$\nu_5 + \nu_6(E) - \nu_5$	1151	164	14	0.70
$2\nu_6(A_1) - \nu_6$	1155	402	17	0.44
$\nu_3 + \nu_6 - \nu_3$	1158	270	15	0.70
$\nu_5 + \nu_6(A_1) - \nu_5$	1161	53	12	0.52
$2\nu_6(E) - \nu_6$	1162	586	19	0.60
$\nu_5 + \nu_6(A_2) - \nu_5$	1163	115	14	0.54
$2\nu_3 - \nu_3$	1291	237	17	0.59
$\nu_3 + \nu_5 - \nu_5$	1304	207	14	0.52
$\nu_3 + \nu_6 - \nu_6$	1304	373	17	0.71
$\nu_5 + \nu_6(E) - \nu_3$	1316	34	13	0.68
$\nu_5 + \nu_6(A_1) - \nu_3$	1326	13	11	0.61
$\nu_5 + \nu_6(A_2) - \nu_3$	1328	9	9	0.47
$2\nu_3 - \nu_6$	1437	19	11	0.74
$2\nu_5(A_1) - \nu_5$	1438	51	10	0.67
$\nu_5 + \nu_6(E) - \nu_6$	1462	246	14	0.64
$2\nu_5(E) - \nu_5$	1468	103	11	0.79
$\nu_3 + \nu_5 - \nu_3$	1469	131	13	0.58
$\nu_5 + \nu_6(A_1) - \nu_6$	1472	64	13	0.58
$\nu_5 + \nu_6(A_2) - \nu_6$	1474	209	12	0.53
$\nu_1 - \nu_5$	1497	2	7	0.55
$\nu_4 - \nu_5$	1545	0	-	-
$2\nu_5(A_1) - \nu_3$	1604	0	-	-
$\nu_3 + \nu_5 - \nu_6$	1615	0	-	-
$2\nu_5(A_1) - \nu_6$	1749	0	-	-
Nonad − Triad (Present Work)		3304	17	0.62
Nonad − Triad (Ref. 16)		2487	15	4.3

Table 6 - Detailed Statistics of the Simultaneous Fit of the Triad, Nonad and Nonad−Triad of CH_3D Nonad Band System

Band	Origin cm^{-1}	Nb Fitted Positions	Jmax	St. Dev. 10^{-3} cm^{-1}	Nb Fitted Intensities	Jmax	St. Dev. %	Nb Calc. Lines	Int. Summation cm/molecule
$\nu_2(E)$	2200.041	588	22	0.61	250	18	2.7 %	1142	$7.85\ 10^{-19}$
$2\nu_6(A_1)$	2316.273	584	19	0.96	206	18	3.4 %	1450	$1.46\ 10^{-19}$
$2\nu_6(E)$	2323.289	1160	20	0.70	280	19	3.3 %	3219	$6.77\ 10^{-20}$
$\nu_3+\nu_6(E)$	2465.458	531	17	0.82	161	14	4.4 %	2244	$1.09\ 10^{-20}$
$2\nu_3(A_1)$	2597.681	382	17	0.79	198	16	3.2 %	1090	$1.96\ 10^{-20}$
$\nu_5+\nu_6(E)$	2623.433	592	15	0.77	232	14	3.9 %	2498	$1.36\ 10^{-20}$
$\nu_5+\nu_6(A_1)$	2633.155	138	15	0.56	69	14	3.2 %	674	$9.37\ 10^{-21}$
$\nu_5+\nu_6(A_2)$	2634.838	354	15	0.77	172	14	3.5 %	1578	$1.41\ 10^{-20}$
$\nu_3+\nu_5(E)$	2776.287	451	16	0.88	138	14	3.0 %	2563	$6.32\ 10^{-20}$
$2\nu_5(A_1)$	2910.120	321	18	0.97	127	16	4.6 %	2257	$5.45\ 10^{-19}$
$2\nu_5(E)$	2940.098	549	18	1.3	169	15	4.2 %	4043	$4.17\ 10^{-19}$
$\nu_1(A_1)$	2969.512	374	18	1.2	124	16	4.2 %	2501	$5.28\ 10^{-19}$
$\nu_4(E)$	3016.713	772	20	0.92	333	18	3.5 %	5125	$6.33\ 10^{-18}$
Nonad (Present Work)		6796	22	0.88	2459	19	3.6 %	30384	$8.95\ 10^{-18}$
Nonad (Ref. 16)		5208	18	4.7	1007	15	4.3 %	24302	$8.65\ 10^{-18}$

Table 7a - Predicted Spectrum of the Nonad of CH_3D (ν_2 region)

Positions (cm^{-1})		Intensities ($cm/molecule$)		Assignment	
Calc	$O-C \times 1000$	Calc	$O-C/C$ %	vibrational	rotational
2198.00288	-0.1	0.154 10^{-20}		$\nu_2(A_1)$	^{Q}Q(7, 3,A_1)
2198.00296		0.154 10^{-20}		$\nu_2(A_1)$	^{Q}Q(7, 3,A_2)
2198.01538	-0.3	0.680 10^{-21}		$\nu_2(A_1)$	^{Q}Q(11, 9,A_1)
2198.01540		0.680 10^{-21}		$\nu_2(A_1)$	^{Q}Q(11, 9,A_2)
2198.03712	0.1	0.731 10^{-22}		$\nu_2(A_1)$	^{Q}Q(16,16,E)
2198.06582	0.1	0.273 10^{-20}		$\nu_2(A_1)$	^{Q}Q(9, 7,E)
2198.11309	0.4	0.223 10^{-23}		$2\nu_6(A_1)$	^{R}P(15, 1,E)
2198.18486		0.191 10^{-20}		$\nu_2(A_1)$	^{Q}Q(10, 9,A_2)
2198.18487	-0.6	0.191 10^{-20}	1.8	$\nu_2(A_1)$	^{Q}Q(10, 9,A_1)
2198.22464	0.6	0.151 10^{-20}	-0.3	$\nu_2(A_1)$	^{Q}Q(11,10,E)
2198.25716		0.151 10^{-21}		$\nu_2(A_1)$	^{Q}Q(15,15,A_2)
2198.25716		0.151 10^{-21}		$\nu_2(A_1)$	^{Q}Q(15,15,A_1)
2198.26897	1.2	0.263 10^{-20}		$\nu_2(A_1)$	^{Q}Q(7, 4,E)
2198.29547	-0.2	0.271 10^{-21}		$\nu_2(A_1)$	^{Q}Q(6, 1,E)
2198.34431		0.341 10^{-20}		$\nu_2(A_1)$	^{Q}Q(8, 6,A_2)
2198.34431	-0.5	0.341 10^{-20}	0.4	$\nu_2(A_1)$	^{Q}Q(8, 6,A_1)
2198.40956	-0.0	0.106 10^{-20}		$\nu_2(A_1)$	^{Q}Q(6, 2,E)
2198.41369		0.450 10^{-22}		$2\nu_6(A_1)$	^{Q}P(14, 7,E)
2198.46282	-0.1	0.297 10^{-21}	2.3	$\nu_2(A_1)$	^{Q}Q(14,14,E)
2198.48718		0.668 10^{-23}		$2\nu_6(A_1)$	^{Q}P(15,12,A_2)
2198.48718		0.668 10^{-23}		$2\nu_6(A_1)$	^{Q}P(15,12,A_1)
2198.59943		0.232 10^{-20}		$\nu_2(A_1)$	^{Q}Q(6, 3,A_2)
2198.59946	-0.0	0.232 10^{-20}		$\nu_2(A_1)$	^{Q}Q(6, 3,A_1)
2198.61005		0.388 10^{-20}		$\nu_2(A_1)$	^{Q}Q(7, 5,E)
2198.62784	0.5	0.324 10^{-20}	4.1	$\nu_2(A_1)$	^{Q}Q(9, 8,E)
2198.65344		0.551 10^{-21}		$\nu_2(A_1)$	^{Q}Q(13,13,E)
2198.80589	0.1	0.401 10^{-21}	1.6	$\nu_2(A_1)$	^{Q}Q(5, 1,E)
2198.83019		0.966 10^{-21}		$\nu_2(A_1)$	^{Q}Q(12,12,A_2)
2198.83019		0.966 10^{-21}		$\nu_2(A_1)$	^{Q}Q(12,12,A_1)
2198.83438	0.8	0.427 10^{-20}		$\nu_2(A_1)$	^{Q}Q(8, 7,E)
2198.86471	0.4	0.394 10^{-20}		$\nu_2(A_1)$	^{Q}Q(6, 4,E)
2198.91969	0.2	0.158 10^{-20}	1.4	$\nu_2(A_1)$	^{Q}Q(5, 2,E)
2198.99410	-0.7	0.160 10^{-20}	2.2	$\nu_2(A_1)$	^{Q}Q(11,11,E)
2199.02537		0.521 10^{-20}		$\nu_2(A_1)$	^{Q}Q(7, 6,A_2)
2199.02537	0.0	0.521 10^{-20}		$\nu_2(A_1)$	^{Q}Q(7, 6,A_1)
2199.10907	0.3	0.344 10^{-20}	1.2	$\nu_2(A_1)$	^{Q}Q(5, 3,A_1)
2199.10908		0.344 10^{-20}		$\nu_2(A_1)$	^{Q}Q(5, 3,A_2)
2199.14798	-0.4	0.249 10^{-20}	1.4	$\nu_2(A_1)$	^{Q}Q(10,10,E)
2199.20475	0.2	0.582 10^{-20}		$\nu_2(A_1)$	^{Q}Q(6, 5,E)
2199.20543		0.356 10^{-20}		$\nu_2(A_1)$	^{Q}Q(9, 9,A_2)
2199.20543		0.356 10^{-20}		$\nu_2(A_1)$	^{Q}Q(9, 9,A_1)
2199.23009	1.1	0.594 10^{-21}		$\nu_2(A_1)$	^{Q}Q(4, 1,E)
2199.32746		0.385 10^{-21}		$2\nu_6(E)$	^{P}Q(10, 9,A_2)
2199.32747		0.385 10^{-21}		$2\nu_6(E)$	^{P}Q(10, 9,A_1)
2199.34364	0.4	0.233 10^{-20}	4.0	$\nu_2(A_1)$	^{Q}Q(4, 2,E)
2199.37363	1.0	0.584 10^{-20}		$\nu_2(A_1)$	^{Q}Q(5, 4,E)
2199.39655	-1.6	0.506 10^{-20}		$\nu_2(A_1)$	^{Q}Q(8, 8,E)
2199.51407		0.652 10^{-20}		$\nu_2(A_1)$	^{Q}Q(7, 7,E)
2199.53260		0.508 10^{-20}		$\nu_2(A_1)$	^{Q}Q(4, 3,A_2)
2199.53260	-1.0	0.508 10^{-20}	0.8	$\nu_2(A_1)$	^{Q}Q(4, 3,A_1)

Table 7a - Predicted Spectrum of the Nonad of CH_3D (ν_2 region) (continued)

Positions (cm^{-1})		Intensities ($cm/molecule$)		Assignment	
Calc	$O-C \times 1000$	Calc	$O-C/C$ %	vibrational	rotational
2199.56872		0.894 10^{-21}		$\nu_2(A_1)$	^{Q}Q(3, 1,E)
2199.61882		0.781 10^{-20}		$\nu_2(A_1)$	^{Q}Q(6, 6,A_1)
2199.61882	0.1	0.781 10^{-20}	-2.2	$\nu_2(A_1)$	^{Q}Q(6, 6,A_2)
2199.68206	-0.0	0.351 10^{-20}	0.6	$\nu_2(A_1)$	^{Q}Q(3, 2,E)
2199.71274	-0.5	0.862 10^{-20}	0.5	$\nu_2(A_1)$	^{Q}Q(5, 5,E)
2199.74723	0.3	0.276 10^{-22}		$2\nu_6(E)$	^{P}P(12, 2,E)
2199.82227	-0.0	0.143 10^{-20}	5.5	$\nu_2(A_1)$	^{Q}Q(2, 1,E)
2199.87068		0.765 10^{-20}		$\nu_2(A_1)$	^{Q}Q(3, 3,A_2)
2199.76658	-0.2	0.187 10^{-21}		$2\nu_6(E)$	^{P}P(6, 6,A_1)
2199.76659		0.187 10^{-21}		$2\nu_6(E)$	^{P}P(6, 6,A_2)
2199.79655	0.8	0.864 10^{-20}		$\nu_2(A_1)$	^{Q}Q(4, 4,E)
2199.87068	-0.6	0.765 10^{-20}	-1.5	$\nu_2(A_1)$	^{Q}Q(3, 3,A_1)
2199.93545	-0.5	0.561 10^{-20}	1.9	$\nu_2(A_1)$	^{Q}Q(2, 2,E)
2199.99110	-0.2	0.277 10^{-20}	1.9	$\nu_2(A_1)$	^{Q}Q(1, 1,E)
2200.12576	0.3	0.368 10^{-22}	-1.0	$2\nu_6(A_1)$	^{Q}P(14, 8,E)
2200.23181	-0.3	0.683 10^{-22}	2.8	$2\nu_6(A_1)$	^{Q}P(14, 0,A_1)
2200.48220	-1.4	0.874 10^{-23}		$2\nu_6(E)$	^{S}P(10, 3,A_1)
2200.48498		0.816 10^{-23}		$2\nu_6(E)$	^{S}P(10, 3,A_2)
2200.72318		0.114 10^{-21}		$2\nu_6(E)$	^{P}Q(9, 9,A_2)
2200.72326		0.113 10^{-21}		$2\nu_6(E)$	^{P}Q(9, 9,A_1)
2200.82037	-0.4	0.566 10^{-22}	1.0	$2\nu_6(A_1)$	^{Q}P(14, 1,E)
2200.94917	-0.3	0.387 10^{-23}		$2\nu_6(E)$	^{R}P(16, 0,A_1)
2200.98406	-0.1	0.940 10^{-22}		$2\nu_6(E)$	^{P}P(9, 4,E)
2200.98967		0.373 10^{-23}		$2\nu_6(A_1)$	^{Q}P(15,13,E)
2201.12379	0.3	0.809 10^{-22}	3.0	$2\nu_6(A_1)$	^{Q}P(13, 3,A_2)
2201.56841	0.4	0.827 10^{-22}	1.2	$2\nu_6(A_1)$	^{Q}P(13, 3,A_1)
2201.70117	-0.1	0.849 10^{-23}	5.3	$2\nu_6(E)$	^{O}P(15, 4,E)
2201.98886		0.286 10^{-22}		$2\nu_6(A_1)$	^{Q}P(14, 9,A_2)
2201.98886	-0.0	0.286 10^{-22}	1.3	$2\nu_6(A_1)$	^{Q}P(14, 9,A_1)

Table 7b - Predicted Spectrum of the Nonad of CH_3D ($\nu_3 + \nu_5$ region)

Positions (cm^{-1})		Intensities ($cm/molecule$)		Assignment	
Calc	$O-C \times 1000$	Calc	$O-C/C$ %	vibrational	rotational
2774.09293		0.726 10^{-23}		$\nu_5+\nu_6(E)$	^{R}R(14, 4,E)
2774.18291	-0.6	0.280 10^{-21}	5.2	$\nu_3+\nu_5(E)$	^{P}Q(4, 1,E)
2774.19012		0.101 10^{-22}		$2\nu_5(A_1)$	^{Q}P(19, 6,A_2)
2774.20932		0.113 10^{-22}		$2\nu_5(A_1)$	^{Q}P(20, 4,E)
2774.24059		0.101 10^{-22}		$2\nu_5(A_1)$	^{Q}P(19, 6,A_1)
2774.27845		0.213 10^{-23}		$\nu_3+\nu_5(E)$	^{S}Q(16, 1,E)
2774.29335		0.133 10^{-22}		$\nu_5+\nu_6(E)$	^{R}R(12, 7,E)
2774.31579		0.187 10^{-22}		$\nu_5+\nu_6(A_2)$	^{Q}R(11, 5, E)
2774.32956	0.7	0.122 10^{-21}		$\nu_3+\nu_5(E)$	^{R}Q(11, 0,A_2)
2774.34469		0.270 10^{-23}		$\nu_3+\nu_5(E)$	^{S}Q(7, 0,A_2)
2774.44833		0.101 10^{-23}		$\nu_5+\nu_6(E)$	^{O}R(18, 3,A_2)
2774.46632	-0.4	0.247 10^{-21}	-3.8	$\nu_3+\nu_5(E)$	^{P}Q(3, 1,E)
2774.53778		0.119 10^{-22}		$2\nu_5(E)$	^{O}P(16, 8,E)
2774.58085		0.320 10^{-23}		$\nu_3+\nu_5(E)$	^{S}Q(15, 1,E)
2774.64803		0.157 10^{-23}		$\nu_5+\nu_6(A_2)$	^{Q}R(14, 1, E)
2774.68645	-0.7	0.194 10^{-21}	4.6	$\nu_3+\nu_5(E)$	^{P}Q(2, 1,E)
2774.69948		0.128 10^{-22}		$\nu_5+\nu_6(E)$	^{R}R(10,10,E)
2774.83737	-0.3	0.124 10^{-21}	3.6	$\nu_3+\nu_5(E)$	^{P}Q(1, 1,E)
2774.87677		0.444 10^{-23}		$\nu_3+\nu_5(E)$	^{S}Q(14, 1,E)
2774.99540		0.147 10^{-23}		$2\nu_5(A_1)$	^{Q}P(18,15,A_2)
2774.99540		0.147 10^{-23}		$2\nu_5(A_1)$	^{Q}P(18,15,A_1)
2775.00257		0.168 10^{-22}		$2\nu_5(E)$	^{O}P(13, 9,A_2)
2775.00258		0.168 10^{-22}		$2\nu_5(E)$	^{O}P(13, 9,A_1)
2775.04701	0.2	0.193 10^{-21}	5.4	$\nu_3+\nu_5(E)$	^{R}Q(10, 0,A_1)
2775.16225		0.209 10^{-23}		$2\nu_5(A_1)$	^{Q}P(21, 9,A_2)
2775.17028		0.566 10^{-23}		$\nu_3+\nu_5(E)$	^{S}Q(13, 1,E)
2775.17496		0.198 10^{-23}		$2\nu_5(A_1)$	^{Q}P(21, 9,A_1)
2775.36746	-0.6	0.135 10^{-22}		$\nu_5+\nu_6(A_2)$	^{Q}R(12, 4,E)
2775.46780	0.3	0.652 10^{-23}		$\nu_3+\nu_5(E)$	^{S}Q(12, 1,E)
2775.51493		0.130 10^{-22}		$2\nu_5(A_1)$	^{Q}P(20, 3,A_2)
2775.59186		0.129 10^{-22}		$2\nu_5(A_1)$	^{Q}P(20, 3,A_1)
2775.62084		0.209 10^{-23}		$\nu_5+\nu_6(E)$	^{R}R(16, 1,E)
2775.71561		0.115 10^{-23}		$2\nu_5(E)$	^{R}P(18,13,E)
2775.77620		0.670 10^{-23}		$\nu_3+\nu_5(E)$	^{S}Q(11, 1,E)
2775.82245	-0.2	0.276 10^{-21}	4.6	$\nu_3+\nu_5(E)$	^{R}Q(9, 0,A_2)
2775.88795		0.288 10^{-23}		$2\nu_5(A_1)$	^{Q}P(20,11,E)
2776.10076	-1.0	0.606 10^{-23}		$\nu_3+\nu_5(E)$	^{S}Q(10, 1,E)
2776.17913		0.141 10^{-23}		$2\nu_5(A_1)$	^{Q}P(19,14,E)
2776.35777		0.146 10^{-22}		$2\nu_5(A_1)$	^{Q}P(20, 2,E)
2776.44322		0.477 10^{-23}		$\nu_3+\nu_5(E)$	^{S}Q(9, 1,E)
2776.61633	-0.5	0.363 10^{-21}	0.8	$\nu_3+\nu_5(E)$	^{R}Q(8, 0,A_1)
2776.77912		0.401 10^{-23}		$\nu_5+\nu_6(E)$	^{R}R(15, 3,A_2)
2776.79491		0.527 10^{-23}		$2\nu_5(E)$	$^?$P(18, 7,E)
2776.79664		0.155 10^{-22}		$2\nu_5(A_1)$	^{Q}P(20, 1,E)
2776.80063		0.323 10^{-23}		$\nu_3+\nu_5(E)$	^{S}Q(8, 1,E)
2776.81522		0.103 10^{-22}		$\nu_5+\nu_6(E)$	^{R}R(13, 6,A_2)
2776.81522		0.103 10^{-22}		$\nu_5+\nu_6(E)$	^{R}R(13, 6,A_1)
2776.83789		0.363 10^{-23}		$\nu_5+\nu_6(E)$	^{R}R(15, 3,A_1)
2776.88920		0.850 10^{-23}		$\nu_5+\nu_6(A_2)$	^{Q}R(13, 3,A_2)
2776.93604		0.158 10^{-22}		$2\nu_5(A_1)$	^{Q}P(20, 0,A_1)

Table 7b - Predicted Spectrum of the Nonad of CH_3D ($\nu_3 + \nu_5$ region) (continued)

Positions (cm^{-1})		Intensities ($cm/molecule$)		Assignment	
Calc	$O-C \times 1000$	Calc	$O-C/C$ %	vibrational	rotational
2777.16544		0.186 10^{-23}		$\nu_3+\nu_5(E)$	^{S}Q(7, 1,E)
2777.16954		0.102 10^{-23}		$\nu_3+\nu_5(E)$	^{S}Q(16, 2,E)
2777.17521		0.800 10^{-23}		$\nu_5+\nu_6(A_2)$	^{Q}R(13, 3,A_1)
2777.25494		0.190 10^{-23}		$2\nu_5(A_1)$	^{Q}P(17,15,A_2)
2777.25494		0.190 10^{-23}		$2\nu_5(A_1)$	^{Q}P(17,15,A_1)
2777.34381		0.132 10^{-22}		$\nu_5+\nu_6(E)$	^{R}R(11, 9,A_2)
2777.34381		0.132 10^{-22}		$\nu_5+\nu_6(E)$	^{R}R(11, 9,A_1)
2777.39033	-1.2	0.446 10^{-21}		$\nu_3+\nu_5(E)$	^{R}Q(7, 0,A_2)
2777.39960		0.131 10^{-23}		$\nu_3+\nu_5(E)$	^{S}Q(15, 2,E)
2777.41419		0.128 10^{-23}		$\nu_5+\nu_6(A_1)$	^{Q}R(17, 2,E)
2777.42061		0.266 10^{-23}		$2\nu_5(A_1)$	^{Q}P(19,12,A_2)
2777.42061		0.266 10^{-23}		$2\nu_5(A_1)$	^{Q}P(19,12,A_1)
2777.64098		0.154 10^{-23}		$\nu_3+\nu_5(E)$	^{S}Q(14, 2,E)
2777.80255	-2.8	0.661 10^{-23}		$2\nu_5(E)$	^{O}P(17, 7,E)
2777.90025		0.165 10^{-23}		$\nu_3+\nu_5(E)$	^{S}Q(13, 2,E)
2778.11523	-1.2	0.512 10^{-21}	-1.0	$\nu_3+\nu_5(E)$	^{R}Q(6, 0,A_1)
2778.18234		0.160 10^{-23}		$\nu_3+\nu_5(E)$	^{S}Q(12, 2,E)
2778.39533		0.265 10^{-23}		$\nu_5+\nu_6(A_1)$	^{Q}R(17, 1,E)
2778.43506		0.108 10^{-23}		$2\nu_5(E)$	^{R}P(17,13,E)
2778.48973		0.141 10^{-23}		$\nu_3+\nu_5(E)$	^{S}Q(11, 2,E)
2778.51215		0.200 10^{-23}		$2\nu_5(E)$	^{P}P(21,21,A_2)
2778.51215		0.200 10^{-23}		$2\nu_5(E)$	^{P}P(21,21,A_1)
2778.53250		0.161 10^{-22}		$2\nu_5(A_1)$	^{Q}P(19, 5,E)
2778.60819		0.179 10^{-23}		$2\nu_5(A_1)$	^{Q}P(16,15,A_2)
2778.60819		0.179 10^{-23}		$2\nu_5(A_1)$	^{Q}P(16,15,A_1)
2778.70738		0.379 10^{-23}		$2\nu_5(A_1)$	^{Q}P(20,10,E)
2778.76965	-1.6	0.550 10^{-21}		$\nu_3+\nu_5(E)$	^{R}Q(5, 0,A_2)
2778.78483		0.168 10^{-22}		$2\nu_5(E)$	^{O}P(15, 8,E)
2778.82196		0.112 10^{-23}		$\nu_3+\nu_5(E)$	^{S}Q(10, 2,E)
2778.89776		0.113 10^{-23}		$\nu_4(E)$	^{P}P(22,20,E)
2778.96508		0.238 10^{-23}		$\nu_1(A_1)$	^{Q}P(21, 8,E)
2779.14518		0.191 10^{-22}		$2\nu_5(E)$	^{O}P(12, 9,A_2)
2779.14518	-0.5	0.191 10^{-22}		$2\nu_5(E)$	^{O}P(12, 9,A_1)
2779.31366		0.408 10^{-23}		$\nu_5+\nu_6(E)$	^{R}R(17, 0,A_2)
2779.33752	-1.1	0.549 10^{-21}	-1.2	$\nu_3+\nu_5(E)$	^{R}Q(4, 0,A_1)
2779.36550		0.104 10^{-23}		$2\nu_5(A_1)$	$^{?}$P(14, 6,A_2)
2779.37498		0.105 10^{-23}		$2\nu_5(A_1)$	$^{?}$P(14, 6,A_1)
2779.44844		0.720 10^{-23}		$\nu_5+\nu_6(E)$	^{R}R(14, 5,E)
2779.74836		0.247 10^{-23}		$2\nu_5(A_1)$	^{Q}P(18,14,E)
2779.77964		0.119 10^{-22}		$\nu_5+\nu_6(E)$	^{R}R(12, 8,E)
2779.80633	-1.0	0.501 10^{-21}	-3.4	$\nu_3+\nu_5(E)$	^{R}Q(3, 0,A_2)
2779.83454		0.381 10^{-23}		$\nu_5+\nu_6(A_2)$	^{Q}R(14, 2,E)
2780.14367		0.171 10^{-23}		$2\nu_5(A_1)$	^{Q}P(19,13,E)
2780.16639	-0.7	0.403 10^{-21}	-2.8	$\nu_3+\nu_5(E)$	^{R}Q(2, 0,A_1)
2780.19080		0.169 10^{-22}		$2\nu_5(A_1)$	^{Q}P(18, 6,A_1)
2780.22406		0.170 10^{-22}		$2\nu_5(A_1)$	^{Q}P(18, 6,A_2)
2780.41046	-0.6	0.262 10^{-21}	-3.4	$\nu_3+\nu_5(E)$	^{R}Q(1, 0,A_2)
2780.50192		0.178 10^{-23}		$\nu_5+\nu_6(E)$	^{R}R(16, 2,E)
2780.78236		0.150 10^{-23}		$\nu_1(A_1)$	$^{?}$P(16, 7,E)
2780.93800		0.144 10^{-22}		$\nu_5+\nu_6(A_1)$	^{Q}R(9, 8,E)

Table 7b - Predicted Spectrum of the Nonad of CH_3D ($\nu_3 + \nu_5$ region) (continued)

Positions (cm^{-1})		Intensities ($cm/molecule$)		Assignment	
Calc	$O-C \times 1000$	Calc	$O-C/C$ %	vibrational	rotational
2780.98591		0.425 10^{-23}		$2\nu_5(A_1)$	^{Q}P(20, 9,A_1)
2780.98710		0.424 10^{-23}		$2\nu_5(A_1)$	^{Q}P(20, 9,A_2)
2780.99776	0.2	0.209 10^{-22}		$2\nu_5(A_1)$	^{Q}P(19, 4,E)
2781.10158		0.485 10^{-23}		$2\nu_5(A_1)$	^{Q}P(19,11,E)
2781.32686		0.318 10^{-23}		$2\nu_5(E)$	^{R}P(18,12,A_2)
2781.32686		0.318 10^{-23}		$2\nu_5(E)$	^{R}P(18,12,A_1)
2781.36610	-0.5	0.181 10^{-22}		$\nu_5 + \nu_6(A_2)$	^{Q}R(10, 7,E)
2781.43753		0.822 10^{-23}		$2\nu_5(E)$	$^{?}$P(17, 7,E)
2781.57045	-0.6	0.111 10^{-23}		$2\nu_5(A_1)$	$^{?}$P(12, 7,E)
2782.01029		0.165 10^{-22}		$\nu_5 + \nu_6(A_2)$	^{Q}R(11, 6,A_2)
2782.01031	-0.3	0.165 10^{-22}		$\nu_5 + \nu_6(A_2)$	^{Q}R(11, 6,A_1)
2782.21293		0.449 10^{-23}		$\nu_5 + \nu_6(E)$	^{R}R(15, 4,E)
2782.23330	0.3	0.957 10^{-23}		$\nu_5 + \nu_6(E)$	^{R}R(13, 7,E)
2782.24377		0.105 10^{-23}		$2\nu_5(A_1)$	$^{?}$P(15, 5,E)
2782.44877		0.249 10^{-22}		$2\nu_5(A_1)$	^{Q}P(19, 3,A_1)
2782.51508	-0.7	0.242 10^{-22}		$2\nu_5(A_1)$	^{Q}P(19, 3,A_2)
2782.74893		0.220 10^{-23}		$\nu_1(A_1)$	^{Q}P(21, 7,E)
2782.81994	-2.0	0.110 10^{-22}		$\nu_5 + \nu_6(E)$	^{R}R(11,10,E)
2782.83190		0.368 10^{-23}		$2\nu_5(A_1)$	^{Q}P(17,14,E)
2782.93167	0.7	0.127 10^{-22}		$\nu_5 + \nu_6(A_2)$	^{Q}R(12, 5,E)
2783.08072		0.135 10^{-23}		$\nu_4(E)$	^{P}P(22,19,E)
2783.09423	1.4	0.221 10^{-22}		$2\nu_5(E)$	^{O}P(14, 8,E)
2783.31490	3.1	0.891 10^{-23}		$2\nu_5(E)$	^{O}P(16, 7,E)
2783.36194		0.194 10^{-22}		$2\nu_5(E)$	^{O}P(11, 9,A_2)
2783.36194		0.194 10^{-22}		$2\nu_5(E)$	^{O}P(11, 9,A_1)
2783.36866		0.120 10^{-23}		$2\nu_5(E)$	$^{?}$P(19, 6,A_1)
2783.37236		0.273 10^{-22}		$2\nu_5(A_1)$	^{Q}P(19, 2,E)
2783.76617		0.370 10^{-22}		$\nu_3 + \nu_5(E)$	^{R}Q(11, 1,E)
2783.78350		0.607 10^{-22}		$\nu_3 + \nu_5(E)$	^{R}Q(10, 1,E)
2783.85405		0.289 10^{-22}		$2\nu_5(A_1)$	^{Q}P(19, 1,E)
2783.88227		0.211 10^{-22}		$\nu_3 + \nu_5(E)$	^{R}Q(12, 1,E)
2783.91583	-0.1	0.930 10^{-22}		$\nu_3 + \nu_5(E)$	^{R}Q(9, 1,E)
2783.96004		0.350 10^{-23}		$2\nu_5(A_1)$	^{Q}P(18,13,E)
2784.00687		0.294 10^{-22}		$2\nu_5(A_1)$	^{Q}P(19, 0,A_2)
2784.04270		0.108 10^{-23}		$\nu_5 + \nu_6(E)$	^{R}R(17, 1,E)
2784.14026	-0.7	0.133 10^{-21}		$\nu_3 + \nu_5(E)$	^{R}Q(8, 1,E)
2784.14488		0.113 10^{-22}		$\nu_3 + \nu_5(E)$	^{R}Q(13, 1,E)
2784.14983		0.710 10^{-23}		$2\nu_5(A_1)$	^{Q}P(19,10,E)
2784.15404		0.247 10^{-23}		$\nu_4(E)$	^{P}P(21,20,E)
2784.27573		0.852 10^{-23}		$\nu_5 + \nu_6(A_2)$	^{Q}R(13, 4,E)
2784.38640		0.150 10^{-23}		$2\nu_5(E)$	^{R}P(19,12,A_2)
2784.38640		0.150 10^{-23}		$2\nu_5(E)$	^{R}P(19,12,A_1)
2784.43084	-0.2	0.175 10^{-21}	0.3	$\nu_3 + \nu_5(E)$	^{R}Q(7, 1,E)
2784.56147		0.569 10^{-23}		$\nu_3 + \nu_5(E)$	^{R}Q(14, 1,E)
2784.66375		0.481 10^{-23}		$\nu_1(A_1)$	^{Q}P(20, 8,E)
2784.75694		0.333 10^{-23}		$2\nu_5(E)$	^{R}P(17,12,A_2)
2784.75694		0.333 10^{-23}		$2\nu_5(E)$	^{R}P(17,12,A_1)
2784.76024	-0.2	0.214 10^{-21}		$\nu_3 + \nu_5(E)$	^{R}Q(6, 1,E)
2784.78259		0.693 10^{-23}		$\nu_5 + \nu_6(E)$	^{R}R(14, 6,A_1)
2784.78260		0.693 10^{-23}		$\nu_5 + \nu_6(E)$	^{R}R(14, 6,A_2)

Table 7b - Predicted Spectrum of the Nonad of CH_3D ($\nu_3 + \nu_5$ region) (continued)

Positions (cm^{-1})		Intensities ($cm/molecule$)		Assignment	
Calc	$O-C \times 1000$	Calc	$O-C/C$ %	vibrational	rotational
2784.79243		0.200 10^{-23}		$\nu_5+\nu_6(E)$	^{R}R(16, 3,A_1)
2784.92179		0.153 10^{-23}		$\nu_5+\nu_6(E)$	^{R}R(16, 3,A_2)
2784.95646	-0.1	0.281 10^{-22}		$2\nu_5(A_1)$	^{Q}P(18, 5,E)
2785.10139	-0.4	0.239 10^{-21}	-0.3	$\nu_3+\nu_5(E)$	^{R}Q(5, 1,E)
2785.13428		0.271 10^{-23}		$\nu_3+\nu_5(E)$	^{R}Q(15, 1,E)
2785.28620	0.5	0.103 10^{-22}		$\nu_5+\nu_6(E)$	^{R}R(12, 9,A_1)
2785.28622		0.103 10^{-22}		$\nu_5+\nu_6(E)$	^{R}R(12, 9,A_2)
2785.33272		0.462 10^{-23}		$2\nu_5(A_1)$	^{Q}P(16,14,E)
2785.42892	-0.6	0.241 10^{-21}		$\nu_3+\nu_5(E)$	^{R}Q(4, 1,E)
2785.69881		0.140 10^{-23}		$2\nu_5(A_1)$	$^?$P(13, 6,A_1)
2785.70310		0.140 10^{-23}		$2\nu_5(A_1)$	$^?$P(13, 6,A_2)
2785.72019	-0.6	0.211 10^{-21}		$\nu_3+\nu_5(E)$	^{R}Q(3, 1,E)
2785.80735		0.709 10^{-23}		$2\nu_5(A_1)$	^{Q}P(18,11,E)
2785.84152		0.169 10^{-23}		$2\nu_5(A_1)$	$^?$P(17, 3,A_2)
2785.86121		0.123 10^{-23}		$\nu_3+\nu_5(E)$	^{R}Q(16, 1,E)
2785.95615	-0.5	0.139 10^{-21}		$\nu_3+\nu_5(E)$	^{R}Q(2, 1,E)
2785.95620		0.121 10^{-22}		$2\nu_5(E)$	$^?$P(16, 7,E)

Table 7c - Predicted Spectrum of the Nonad of CH_3D (ν_4 region)

Positions (cm^{-1})		Intensities ($cm/molecule$)		Assignment	
Calc	$O-C \times 1000$	Calc	$O-C/C$ %	vibrational	rotational
3076.00996		0.211 10^{-23}		$\nu_4(E)$	^{Q}R(7, 2,E)
3076.04847		0.107 10^{-22}		$2\nu_5(E)$	^{R}R(15, 4,E)
3076.06087	-1.2	0.596 10^{-22}		$2\nu_5(A_1)$	$^{?}$R(12, 5,E)
3076.08572		0.157 10^{-22}		$2\nu_5(A_1)$	^{Q}R(19, 6,A_2)
3076.17764		0.164 10^{-22}		$2\nu_5(A_1)$	^{Q}R(19, 6,A_1)
3076.28587	-0.4	0.914 10^{-20}		$\nu_4(E)$	^{P}R(7, 1,E)
3076.31857	0.9	0.174 10^{-20}		$\nu_4(E)$	^{P}R(8, 5,E)
3076.36280		0.744 10^{-22}		$2\nu_5(A_1)$	^{Q}R(18, 1,E)
3076.44421		0.276 10^{-22}		$\nu_1(A_1)$	$^{?}$R(14, 3,A_1)
3076.44968		0.291 10^{-19}		$\nu_4(E)$	^{R}R(6, 3,A_2)
3076.44973	-0.1	0.291 10^{-19}		$\nu_4(E)$	^{R}R(6, 3,A_1)
3076.45910		0.609 10^{-22}		$\nu_4(E)$	^{P}R(9, 9,A_2)
3076.45910		0.609 10^{-22}		$\nu_4(E)$	^{P}R(9, 9,A_1)
3076.51136		0.753 10^{-22}		$2\nu_5(A_1)$	^{Q}R(18, 0,A_1)
3076.53679		0.806 10^{-22}		$\nu_4(E)$	^{O}R(13, 8,E)
3076.60740		0.313 10^{-22}		$2\nu_5(E)$	^{R}R(15, 5,E)
3076.62563		0.128 10^{-23}		$\nu_1(A_1)$	^{O}R(13, 4,E)
3076.64012		0.136 10^{-21}		$2\nu_5(E)$	^{S}R(9, 3,A_1)
3076.64026		0.137 10^{-21}		$2\nu_5(E)$	^{S}R(9, 3,A_2)
3076.66937		0.212 10^{-23}		$2\nu_5(E)$	$^{?}$R(12, 3,A_2)
3076.66954		0.220 10^{-23}		$2\nu_5(E)$	$^{?}$R(12, 3,A_1)
3076.86007		0.381 10^{-22}		$\nu_4(E)$	^{O}R(11, 6,A_1)
3076.86185		0.381 10^{-22}		$\nu_4(E)$	^{O}R(11, 6,A_2)
3076.90706		0.131 10^{-21}		$2\nu_5(E)$	^{R}R(13, 2,E)
3076.92203		0.391 10^{-23}		$2\nu_5(A_1)$	^{Q}R(20, 8,E)
3076.94406		0.312 10^{-23}		$\nu_1(A_1)$	$^{?}$R(8, 3,A_2)
3076.94407		0.311 10^{-23}		$\nu_1(A_1)$	$^{?}$R(8, 3,A_1)
3076.97563		0.942 10^{-23}		$2\nu_5(E)$	$^{?}$R(18, 6,A_2)
3076.98591		0.122 10^{-23}		$2\nu_5(E)$	^{S}Q(17, 7,E)
3077.00389		0.670 10^{-23}		$\nu_1(A_1)$	$^{?}$R(15, 6,A_2)
3077.01087		0.402 10^{-23}		$2\nu_5(A_1)$	$^{?}$R(16, 1,E)
3077.20287	6.0	0.366 10^{-21}		$2\nu_5(E)$	$^{?}$R(13, 1,E)
3077.23634	1.7	0.194 10^{-21}		$\nu_1(A_1)$	^{Q}R(12, 7,E)
3077.24384		0.608 10^{-22}		$\nu_4(E)$	^{S}R(6, 0,A_1)
3077.31133		0.134 10^{-22}		$\nu_1(A_1)$	^{Q}R(14,14,E)
3077.36024		0.300 10^{-22}		$2\nu_5(A_1)$	^{Q}R(18,10,E)
3077.42794		0.408 10^{-23}		$2\nu_5(A_1)$	^{Q}R(19,15,A_2)
3077.42794		0.408 10^{-23}		$2\nu_5(A_1)$	^{Q}R(19,15,A_1)
3077.56416		0.690 10^{-23}		$\nu_1(A_1)$	$^{?}$R(15, 6,A_1)
3077.61345		0.664 10^{-23}		$2\nu_5(A_1)$	^{Q}R(19,13,E)
3077.64786		0.299 10^{-23}		$\nu_4(E)$	^{S}Q(15, 8,E)
3077.97993		0.496 10^{-23}		$2\nu_5(E)$	$^{?}$R(8, 0,A_1)
3077.99564		0.843 10^{-22}		$\nu_1(A_1)$	^{Q}R(17, 7,E)
3078.05755		0.320 10^{-22}		$\nu_1(A_1)$	^{Q}R(13,11,E)
3078.18036	-0.8	0.278 10^{-20}		$\nu_4(E)$	^{P}R(8, 4,E)
3078.18327		0.664 10^{-23}		$2\nu_5(E)$	$^{?}$R(18, 6,A_1)
3078.18582		0.270 10^{-21}		$\nu_1(A_1)$	^{Q}R(13, 9,A_2)
3078.18582		0.270 10^{-21}		$\nu_1(A_1)$	^{Q}R(13, 9,A_1)
3078.26547		0.108 10^{-23}		$2\nu_5(E)$	^{O}R(21, 9,A_1)
3078.27275		0.290 10^{-23}		$2\nu_5(E)$	^{R}R(17,10,E)

Table 7c - Predicted Spectrum of the Nonad of CH_3D (ν_4 region) (continued)

Positions (cm^{-1})		Intensities ($cm/molecule$)		Assignment	
Calc	$O-C \times 1000$	Calc	$O-C/C$ %	vibrational	rotational
3078.27424		0.107 10^{-23}		$2\nu_5(E)$	^{O}R(21, 9,A_2)
3078.31219	0.4	0.261 10^{-19}	-4.1	$\nu_4(E)$	^{R}R(7, 0,A_2)
3078.35422	-0.1	0.336 10^{-19}		$\nu_4(E)$	^{R}R(6, 4,E)
3078.38312		0.455 10^{-23}		$\nu_4(E)$	^{O}R(14, 9,A_1)
3078.38314		0.455 10^{-23}		$\nu_4(E)$	^{O}R(14, 9,A_2)
3078.41846	0.2	0.218 10^{-21}		$\nu_4(E)$	^{P}R(9, 8,E)
3078.48153		0.488 10^{-22}		$\nu_4(E)$	^{Q}R(7, 1,E)
3078.49259		0.161 10^{-22}		$2\nu_5(A_1)$	$^{?}$R(13, 3,A_1)
3078.50311		0.238 10^{-22}		$2\nu_5(A_1)$	$^{?}$R(13, 3,A_2)
3078.53008	0.7	0.632 10^{-21}	7.3	$\nu_1(A_1)$	^{Q}R(12, 4,E)
3078.54365		0.130 10^{-22}		$\nu_4(E)$	^{O}R(12, 7,E)
3078.57053		0.188 10^{-21}		$2\nu_5(E)$	^{P}R(12, 2,E)
3078.64128		0.710 10^{-23}		$2\nu_5(E)$	^{P}R(15,15,A_2)
3078.64128		0.710 10^{-23}		$2\nu_5(E)$	^{P}R(15,15,A_1)
3078.77667		0.281 10^{-23}		$2\nu_5(E)$	^{O}R(20, 7,E)
3078.77923	0.3	0.321 10^{-21}		$2\nu_5(E)$	$^{?}$R(13, 1,E)
3078.93838		0.496 10^{-23}		$2\nu_5(A_1)$	$^{?}$R(17, 0,A_2)
3078.95993		0.194 10^{-23}		$\nu_1(A_1)$	$^{?}$R(17, 5,E)
3079.04934		0.112 10^{-22}		$\nu_1(A_1)$	$^{?}$R(9, 2,E)
3079.05146		0.124 10^{-21}		$\nu_1(A_1)$	^{Q}R(12, 6,A_2)
3079.05281	0.6	0.124 10^{-21}		$\nu_1(A_1)$	^{Q}R(12, 6,A_1)
3079.11593		0.769 10^{-22}		$\nu_1(A_1)$	^{Q}R(14,12,A_2)
3079.11593		0.769 10^{-22}		$\nu_1(A_1)$	^{Q}R(14,12,A_1)
3079.15322		0.609 10^{-23}		$2\nu_5(E)$	^{R}R(18,12,A_2)
3079.15322		0.609 10^{-23}		$2\nu_5(E)$	^{R}R(18,12,A_1)
3079.47317	-0.5	0.865 10^{-21}		$\nu_1(A_1)$	^{Q}R(13, 0,A_2)
3079.68264		0.348 10^{-22}		$\nu_4(E)$	^{O}R(8, 2,E)
3079.68345	-0.9	0.117 10^{-21}		$2\nu_5(E)$	^{O}R(15, 4,E)
3079.70534		0.139 10^{-23}		$\nu_4(E)$	^{S}Q(11, 9,A_2)
3079.70534		0.139 10^{-23}		$\nu_4(E)$	^{S}Q(11, 9,A_1)
3079.72170		0.254 10^{-22}		$2\nu_5(A_1)$	^{Q}R(19, 5,E)
3079.77104	0.4	0.299 10^{-21}		$2\nu_5(E)$	^{S}R(8, 5,E)
3079.81485		0.434 10^{-22}		$2\nu_5(A_1)$	^{Q}R(18, 9,A_1)
3079.81604		0.434 10^{-22}		$2\nu_5(A_1)$	^{Q}R(18, 9,A_2)
3079.83700		0.569 10^{-23}		$2\nu_5(A_1)$	$^{?}$R(12, 0,A_1)
3079.87032	0.5	0.860 10^{-22}		$\nu_1(A_1)$	^{Q}R(16, 5,E)
3079.88388		0.132 10^{-23}		$2\nu_5(A_1)$	^{R}R(18, 1,E)

Appendix - Effective Hamiltonian Terms for the Nonad of CH_3D

	Tensorial Nomenclature		Parameter value	
	Rotational	Vibrational	Computer Input	Rounded (St. Dev.)
		Groud State parameters		
1	R2(0,0A$_1$)	000000 000000	0.43370639882E+01	fixed
2	R2(2,0A$_1$)	000000 000000	0.27976669802E+00	fixed
3	R4(0,0A$_1$)	000000 000000	-0.78980213575E-04	fixed
4	R4(2,0A$_1$)	000000 000000	0.51922679070E-05	fixed
5	R4(4,0A$_1$)	000000 000000	0.23599868612E-05	fixed
6	R4(4,3A$_1$)	000000 000000	-0.63131101047E-06	fixed
7	R6(0,0A$_1$)	000000 000000	0.39014875187E-08	fixed
8	R6(2,0A$_1$)	000000 000000	0.20045260285E-09	fixed
9	R6(4,0A$_1$)	000000 000000	0.11777289749E-09	fixed
10	R6(4,3A$_1$)	000000 000000	0.76905950944E-09	fixed
11	R6(6,0A$_1$)	000000 000000	-0.63420687584E-11	fixed
12	R6(6,6A$_1$)	000000 000000	0.45516011795E-11	fixed
13	R8(0,0A$_1$)	000000 000000	-0.17843466965E-12	fixed
14	R8(2,0A$_1$)	000000 000000	0.42845664335E-14	fixed
15	R8(4,0A$_1$)	000000 000000	0.15040841452E-13	fixed
16	R8(6,0A$_1$)	000000 000000	-0.13098408786E-14	fixed
17	R8(6,6A$_1$)	000000 000000	-0.39402595781E-14	fixed
		Triad parameters		
18	R0(0,0A$_1$)	001000 001000	0.13068476597E+04	1306.847660(31)
19	R2(2,0A$_1$)	001000 001000	0.72293335985E-02	7.2292(61) 10^{-3}
20	R4(0,0A$_1$)	001000 001000	-0.71088869160E-05	-7.06(11) 10^{-6}
21	R4(2,0A$_1$)	001000 001000	0.69667744801E-06	6.88(28) 10^{-7}
22	R4(4,0A$_1$)	001000 001000	0.11929438709E-05	1.180(26) 10^{-6}
23	R4(4,3A$_1$)	001000 001000	0.33213344498E-05	3.328(88) 10^{-6}
24	R6(0,0A$_1$)	001000 001000	0.23826719800E-08	2.389(53) 10^{-9}
25	R6(4,3A$_1$)	001000 001000	-0.13092278465E-08	-1.307(50) 10^{-9}
26	R6(6,0A$_1$)	001000 001000	-0.13717597346E-09	-1.375(30) 10^{-10}
27	R6(6,3A$_1$)	001000 001000	0.11164807450E-08	1.112(30) 10^{-9}
28	R6(6,6A$_1$)	001000 001000	0.36235730169E-09	3.59(24) 10^{-10}
29	R1(1,1E)	001000 000010	-0.43616969908E+01	-4.36171(23)
30	R2(2,1E)	001000 000010	0.66927163477E-03	6.78(75) 10^{-4}
31	R2(2,2E)	001000 000010	-0.43035262783E-02	-4.35(17) 10^{-3}
32	R3(1,1E)	001000 000010	-0.15956110485E-03	-1.5905(88) 10^{-4}
33	R3(3,1E)	001000 000010	0.32062698596E-03	3.198(20) 10^{-4}
34	R3(3,2E)	001000 000010	-0.12663151403E-03	-1.258(21) 10^{-4}
35	R4(2,1E)	001000 000010	0.27371355740E-05	2.721(38) 10^{-6}
36	R4(4,4E)	001000 000010	0.10903238956E-05	1.130(84) 10^{-6}
37	R5(5,1E)	001000 000010	-0.61822997280E-08	-6.10(65) 10^{-9}
38	R5(5,2E)	001000 000010	0.16994359432E-07	1.77(20) 10^{-8}
39	R5(5,4E)	001000 000010	0.70244443844E-07	6.90(21) 10^{-8}
40	R5(5,5E)	001000 000010	-0.15556181916E-07	-1.50(13) 10^{-8}
41	R6(4,1E)	001000 000010	0.43598218350E-09	4.30(26) 10^{-10}
42	R6(4,4E)	001000 000010	-0.11685002461E-08	-1.156(45) 10^{-9}
43	R6(6,1E)	001000 000010	0.53654114295E-09	5.32(11) 10^{-10}
44	R6(6,2E)	001000 000010	-0.40267015417E-09	-4.05(26) 10^{-10}
45	R6(6,5E)	001000 000010	0.97662899894E-09	9.62(62) 10^{-10}
46	R1(1,1E)	001000 000001	0.20262337644E+01	2.02625(33)
47	R2(2,1E)	001000 000001	-0.52094697611E-02	-5.22(21) 10^{-3}
48	R3(3,1E)	001000 000001	-0.91872612179E-04	-9.23(31) 10^{-5}

Appendix - Effective Hamiltonian Terms for the Nonad of CH_3D (Continued)

	Tensorial Nomenclature		Parameter value	
	Rotational	Vibrational	Computer Input	Rounded (St. Dev.)
49	R4(2,2E)	001000 000001	-0.80978330322E-06	-8.08(50) 10^{-7}
50	R4(4,2E)	001000 000001	0.69055936069E-05	6.901(60) 10^{-6}
51	R5(5,4E)	001000 000001	-0.70451406911E-07	-7.18(24) 10^{-8}
52	R5(5,5E)	001000 000001	0.38559443715E-07	3.85(10) 10^{-8}
53	R6(2,1E)	001000 000001	0.77723669302E-09	7.83(31) 10^{-10}
54	R6(4,2E)	001000 000001	0.89374295108E-09	9.10(34) 10^{-10}
55	R6(4,4E)	001000 000001	-0.50838674404E-09	-5.13(35) 10^{-10}
56	R6(6,2E)	001000 000001	0.50547722426E-09	4.98(22) 10^{-10}
57	R6(6,4E)	001000 000001	-0.52387651247E-09	-5.16(36) 10^{-10}
58	R0(0,0A_1)	000010 000010	0.14720223386E+04	1472.022339(21)
59	R1(1,0A_2)	000010 000010	0.19059397914E+01	1.905940(58)
60	R2(0,0A_1)	000010 000010	-0.48791580854E-02	-4.87912(65) 10^{-3}
61	R2(2,0A_1)	000010 000010	-0.17786332331E-01	-1.7786(80) 10^{-2}
62	R2(2,1E)	000010 000010	0.35375198968E-01	3.535(10) 10^{-2}
63	R3(3,0A_2)	000010 000010	-0.11685119978E-03	-1.170(12) 10^{-4}
64	R3(3,3A_2)	000010 000010	-0.92701122345E-04	-9.25(26) 10^{-5}
65	R4(0,0A_1)	000010 000010	-0.14109707722E-05	-1.426(39) 10^{-6}
66	R4(2,0A_1)	000010 000010	-0.20137684971E-05	-2.006(24) 10^{-6}
67	R4(4,0A_1)	000010 000010	-0.58771087979E-06	-5.75(23) 10^{-7}
68	R4(4,3A_1)	000010 000010	-0.45935623173E-05	-4.570(91) 10^{-6}
69	R5(3,0A_2)	000010 000010	0.44883776949E-08	4.497(51) 10^{-9}
70	R5(5,3A_2)	000010 000010	0.42602846887E-07	4.31(16) 10^{-8}
71	R6(2,1E)	000010 000010	-0.71352697078E-09	-7.18(31) 10^{-10}
72	R6(2,2E)	000010 000010	0.13280075223E-08	1.323(37) 10^{-9}
73	R6(4,0A_1)	000010 000010	0.86336510403E-10	8.57(23) 10^{-11}
74	R6(4,3A_1)	000010 000010	-0.25583736650E-08	-2.503(68) 10^{-9}
75	R6(4,1E)	000010 000010	-0.33810465865E-09	-3.43(30) 10^{-10}
76	R6(4,4E)	000010 000010	-0.50042357951E-09	-5.06(42) 10^{-10}
77	R6(6,0A_1)	000010 000010	0.16216584075E-09	1.623(33) 10^{-10}
78	R6(6,6A_1)	000010 000010	-0.38886392632E-09	-3.86(18) 10^{-10}
79	R6(6,1E)	000010 000010	-0.28773183471E-09	-2.92(17) 10^{-10}
80	R6(6,2E)	000010 000010	-0.12918494552E-08	-1.291(49) 10^{-9}
81	R6(6,4E)	000010 000010	0.15457642507E-08	1.539(49) 10^{-9}
82	R6(6,5E)	000010 000010	-0.38213207753E-08	-3.828(64) 10^{-9}
83	R1(1,0A_2)	000010 000001	-0.15674390220E+01	-1.5673(90)
84	R1(1,1E)	000010 000001	0.31382159585E+01	3.1382(85)
85	R2(2,0A_1)	000010 000001	-0.85429912072E-02	-8.55(20) 10^{-3}
86	R2(2,2E)	000010 000001	0.16237055148E-01	1.618(20) 10^{-2}
87	R3(3,3A_1)	000010 000001	-0.74578262949E-04	-7.46(18) 10^{-5}
88	R3(3,1E)	000010 000001	0.13493966637E-03	1.361(50) 10^{-4}
89	R3(3,2E)	000010 000001	0.29236265388E-03	2.898(72) 10^{-4}
90	R4(0,0A_1)	000010 000001	0.15413682927E-05	1.533(35) 10^{-6}
91	R4(2,2E)	000010 000001	0.97544815002E-06	9.48(75) 10^{-7}
92	R4(4,0A_1)	000010 000001	0.79407202576E-06	8.04(30) 10^{-7}
93	R4(4,3A_1)	000010 000001	-0.52510274187E-05	-5.26(11) 10^{-6}
94	R4(4,2E)	000010 000001	0.78970523114E-06	7.8(13) 10^{-7}
95	R4(4,4E)	000010 000001	-0.15807824644E-05	-1.581(99) 10^{-6}
96	R5(3,3A_1)	000010 000001	-0.43950339969E-07	-4.38(15) 10^{-8}
97	R5(3,0A_2)	000010 000001	0.19584594035E-07	1.962(37) 10^{-8}
98	R5(3,3A_2)	000010 000001	-0.29536947405E-07	-2.94(17) 10^{-8}

Appendix - Effective Hamiltonian Terms for the Nonad of CH_3D (Continued)

	Tensorial Nomenclature		Parameter value	
	Rotational	Vibrational	Computer Input	Rounded (St. Dev.)
99	R5(3,1E)	000010 000001	0.16027450275E-07	1.596(54) 10^{-8}
100	R5(3,2E)	000010 000001	0.82533535136E-07	8.06(43) 10^{-8}
101	R5(5,3A_2)	000010 000001	-0.24233860642E-07	-2.37(15) 10^{-8}
102	R5(5,1E)	000010 000001	0.66996109658E-08	6.17(64) 10^{-9}
103	R5(5,2E)	000010 000001	-0.37151408789E-07	-3.67(19) 10^{-8}
104	R5(5,5E)	000010 000001	-0.21931779988E-07	-2.17(10) 10^{-8}
105	R6(0,0A_1)	000010 000001	0.46074501797E-09	4.62(17) 10^{-10}
106	R6(2,0A_1)	000010 000001	0.53916870527E-09	5.37(16) 10^{-10}
107	R6(2,1E)	000010 000001	0.38009214371E-09	3.85(23) 10^{-10}
108	R6(4,0A_1)	000010 000001	0.18517898093E-09	1.80(15) 10^{-10}
109	R6(4,3A_1)	000010 000001	-0.15374242768E-08	-1.523(59) 10^{-9}
110	R6(4,1E)	000010 000001	0.34712687590E-09	3.58(29) 10^{-10}
111	R6(6,0A_1)	000010 000001	0.20496596104E-09	2.039(90) 10^{-10}
112	R6(6,3A_2)	000010 000001	-0.81136083702E-09	-8.15(37) 10^{-10}
113	R6(6,1E)	000010 000001	-0.31454213909E-09	-3.06(14) 10^{-10}
114	R6(6,2E)	000010 000001	0.42409408481E-09	4.36(25) 10^{-10}
115	R6(6,4E)	000010 000001	-0.20148864181E-08	-2.003(45) 10^{-9}
116	R0(0,0A_1)	000001 000001	0.11611028152E+04	1161.102812(21)
117	R1(1,0A_2)	000001 000001	-0.44018667665E+01	-4.401866(57)
118	R2(2,0A_1)	000001 000001	0.14219940149E-01	1.4219(76) 10^{-2}
119	R2(2,1E)	000001 000001	-0.11980417018E-01	-1.193(28) 10^{-2}
120	R2(2,2E)	000001 000001	0.21449004201E-01	2.14493(51) 10^{-2}
121	R3(1,0A_2)	000001 000001	-0.16728937362E-03	-1.673(12) 10^{-4}
122	R3(3,0A_2)	000001 000001	0.27277475381E-04	2.73(11) 10^{-5}
123	R4(0,0A_1)	000001 000001	0.22331943429E-05	2.227(38) 10^{-6}
124	R4(2,0A_1)	000001 000001	0.18560597578E-05	1.855(16) 10^{-6}
125	R4(2,2E)	000001 000001	0.19426096845E-05	1.949(37) 10^{-6}
126	R4(4,3A_1)	000001 000001	0.26890567077E-05	2.703(76) 10^{-6}
127	R4(4,1E)	000001 000001	0.20484129723E-05	2.099(96) 10^{-6}
128	R4(4,4E)	000001 000001	0.16040540990E-05	1.604(19) 10^{-6}
129	R5(3,3A_2)	000001 000001	-0.39036382752E-07	-3.79(14) 10^{-8}
130	R5(5,3A_2)	000001 000001	0.30373563099E-07	2.84(21) 10^{-8}
131	R6(0,0A_1)	000001 000001	-0.84775433624E-09	-8.51(27) 10^{-10}
132	R6(4,1E)	000001 000001	0.57023579213E-09	5.74(66) 10^{-10}
133	R6(4,4E)	000001 000001	0.11906376688E-08	1.157(58) 10^{-9}
134	R6(6,3A_1)	000001 000001	0.44005924744E-09	4.41(27) 10^{-10}
135	R6(6,4E)	000001 000001	-0.12553261858E-08	-1.203(69) 10^{-9}
136	R6(6,5E)	000001 000001	0.33454880022E-09	3.32(30) 10^{-10}
			Nonad parameters	
137	R0(0,0A_1)	100000 100000	0.29692724532E+04	2969.267(12)
138	R2(0,0A_1)	100000 100000	-0.12838198442E-01	-1.2868(98) 10^{-2}
139	R2(2,0A_1)	100000 100000	-0.12353431873E-01	-1.2340(37) 10^{-2}
140	R4(2,0A_1)	100000 100000	-0.32873075051E-05	-3.290(70) 10^{-6}
141	R4(4,0A_1)	100000 100000	-0.23328645638E-05	-2.318(85) 10^{-6}
142	R6(0,0A_1)	100000 100000	0.21836965171E-07	2.175(43) 10^{-8}
143	R6(2,0A_1)	100000 100000	-0.49964806396E-09	-5.03(38) 10^{-10}
144	R6(4,0A_1)	100000 100000	0.13125846619E-08	1.311(42) 10^{-9}
145	R6(6,6A_1)	100000 100000	-0.47255646300E-09	-4.65(23) 10^{-10}
146	R1(1,1E)	100000 001010	0.21320570150E+01	2.1287(65)
147	R2(2,1E)	100000 001010	-0.14559464144E-01	-1.463(32) 10^{-2}

Appendix - Effective Hamiltonian Terms for the Nonad of CH_3D (Continued)

	Tensorial Nomenclature		Parameter value	
	Rotational	Vibrational	Computer Input	Rounded (St. Dev.)
148	R2(2,2E)	100000 001010	-0.24414583445E-01	-2.438(23) 10^{-2}
149	R3(3,1E)	100000 001010	-0.59420079310E-03	-5.94(10) 10^{-4}
150	R3(3,2E)	100000 001010	0.18448720205E-03	1.82(14) 10^{-4}
151	R4(2,1E)	100000 001010	0.50694656217E-05	5.11(33) 10^{-6}
152	R4(2,2E)	100000 001010	-0.65772106615E-05	-6.56(23) 10^{-6}
153	R4(4,1E)	100000 001010	0.39497107275E-05	3.89(17) 10^{-6}
154	R4(4,2E)	100000 001010	0.81541790777E-05	8.17(22) 10^{-6}
155	R1(1,1E)	100000 000100	0.17157436887E+00	1.703(70) 10^{-1}
156	R3(1,1E)	100000 000100	-0.12527290418E-03	-1.281(66) 10^{-4}
157	R3(3,1E)	100000 000100	-0.33068696244E-03	-3.289(70) 10^{-4}
158	R4(2,1E)	100000 000100	-0.10533393378E-04	-1.028(48) 10^{-5}
159	R4(2,2E)	100000 000100	0.75278466483E-05	7.47(25) 10^{-6}
160	R4(4,1E)	100000 000100	0.44286517990E-05	4.42(18) 10^{-6}
161	R4(4,2E)	100000 000100	-0.47473999891E-05	-4.75(13) 10^{-6}
162	R4(4,4E)	100000 000100	0.18139847428E-05	1.787(85) 10^{-6}
163	R5(3,1E)	100000 000100	-0.11318915450E-06	-1.138(77) 10^{-7}
164	R5(3,2E)	100000 000100	0.17388357789E-06	1.72(11) 10^{-7}
165	R5(5,2E)	100000 000100	0.21585191649E-06	2.163(75) 10^{-7}
166	R5(5,4E)	100000 000100	0.43433242603E-07	4.26(49) 10^{-8}
167	R5(5,5E)	100000 000100	-0.85654866273E-07	-8.54(26) 10^{-8}
168	R6(2,1E)	100000 000100	-0.12448140775E-07	-1.233(27) 10^{-8}
169	R6(2,2E)	100000 000100	0.12987557214E-07	1.293(19) 10^{-8}
170	R6(4,1E)	100000 000100	-0.15655894292E-08	-1.58(23) 10^{-9}
171	R6(4,2E)	100000 000100	-0.10470077764E-07	-1.042(28) 10^{-8}
172	R6(6,1E)	100000 000100	-0.48719684183E-09	-4.81(58) 10^{-10}
173	R6(6,2E)	100000 000100	-0.36253199949E-08	-3.61(16) 10^{-9}
174	R6(6,4E)	100000 000100	0.37267009961E-08	3.67(12) 10^{-9}
175	R6(6,5E)	100000 000100	-0.36746608329E-08	-3.66(14) 10^{-9}
176	R0(0,0A_1)	100000 000020	0.38100070702E+01	3.848(98)
177	R2(0,0A_1)	100000 000020	-0.81390478931E-02	-8.164(77) 10^{-3}
178	R2(2,0A_1)	100000 000020	-0.10481272199E-01	-1.0473(73) 10^{-2}
179	R4(0,0A_1)	100000 000020	-0.14825689321E-05	-1.496(54) 10^{-6}
180	R4(2,0A_1)	100000 000020	-0.21277517132E-05	-2.113(83) 10^{-6}
181	R4(4,0A_1)	100000 000020	-0.39748402191E-05	-3.970(74) 10^{-6}
182	R2(2,1E)	100000 000020	0.16190419658E-01	1.617(15) 10^{-2}
183	R3(3,1E)	100000 000020	-0.10212730306E-03	-1.020(54) 10^{-4}
184	R4(4,2E)	100000 000020	-0.57130221493E-05	-5.65(19) 10^{-6}
185	R4(4,4E)	100000 000020	0.22676933306E-05	2.261(34) 10^{-6}
186	R0(0,0A_1)	010000 010000	0.22000377513E+04	2200.03774(14)
187	R2(0,0A_1)	010000 010000	-0.29375436204E-01	-2.93740(47) 10^{-2}
188	R2(2,0A_1)	010000 010000	0.76398119307E-02	7.6399(14) 10^{-3}
189	R4(0,0A_1)	010000 010000	-0.13216969294E-05	-1.332(42) 10^{-6}
190	R4(2,0A_1)	010000 010000	-0.40213298748E-06	-3.98(13) 10^{-7}
191	R4(4,0A_1)	010000 010000	0.41336630711E-06	4.12(13) 10^{-7}
192	R6(0,0A_1)	010000 010000	0.31938201186E-08	3.216(78) 10^{-9}
193	R6(4,0A_1)	010000 010000	-0.14682650190E-09	-1.440(61) 10^{-10}
194	R6(6,6A_1)	010000 010000	-0.61210365761E-10	-6.04(26) 10^{-11}
195	R2(2,0A_1)	010000 000002	0.95327913410E-02	9.51(12) 10^{-3}
196	R3(3,3A_1)	010000 000002	-0.80646238976E-04	-8.01(18) 10^{-5}
197	R4(2,0A_1)	010000 000002	-0.15697051320E-05	-1.558(39) 10^{-6}

Appendix - Effective Hamiltonian Terms for the Nonad of CH_3D (Continued)

	Tensorial Nomenclature		Parameter value	
	Rotational	Vibrational	Computer Input	Rounded (St. Dev.)
198	R4(4,3A$_1$)	010000 000002	0.29787770155E-05	2.970(44) 10^{-6}
199	R1(1,1E)	010000 000002	-0.21278877813E+00	-2.132(17) 10^{-1}
200	R2(2,2E)	010000 000002	0.11374563563E-01	1.142(15) 10^{-2}
201	R3(1,1E)	010000 000002	-0.27968927452E-03	-2.816(39) 10^{-4}
202	R3(3,1E)	010000 000002	0.12378032493E-03	1.247(34) 10^{-4}
203	R3(3,2E)	010000 000002	-0.97047573727E-04	-9.62(27) 10^{-5}
204	R4(2,1E)	010000 000002	0.56602210825E-05	5.71(13) 10^{-6}
205	R4(4,4E)	010000 000002	0.64009643000E-06	6.36(13) 10^{-7}
206	R0(0,0A$_1$)	002000 002000	-0.15133871276E+02	-15.1303(98)
207	R2(0,0A$_1$)	002000 002000	0.12108310150E-01	1.2137(54) 10^{-2}
208	R2(2,0A$_1$)	002000 002000	-0.39237549413E-02	-3.925(12) 10^{-3}
209	R4(4,0A$_1$)	002000 002000	-0.53830119169E-06	-5.26(17) 10^{-7}
210	R4(4,3A$_1$)	002000 002000	-0.30996499885E-05	-3.14(11) 10^{-6}
211	R2(2,2E)	002000 001001	-0.13805316926E-01	-1.363(19) 10^{-2}
212	R3(1,1E)	002000 001001	-0.27076262440E-03	-2.697(29) 10^{-4}
213	R3(3,1E)	002000 001001	-0.32665946422E-04	-3.10(20) 10^{-5}
214	R3(3,2E)	002000 001001	-0.33684123899E-03	-3.326(59) 10^{-4}
215	R0(0,0A$_1$)	002000 000011	0.55096538443E+01	5.520(30)
216	R1(1,0A$_2$)	002000 000011	-0.10351907841E+00	-1.047(43) 10^{-1}
217	R1(1,1E)	002000 000011	0.49474053107E+00	4.956(29) 10^{-1}
218	R2(0,0A$_1$)	002000 000011	-0.80463551915E-02	-8.02(10) 10^{-3}
219	R2(2,2E)	002000 000011	0.82737326727E-02	8.303(93) 10^{-3}
220	R3(1,0A$_2$)	002000 000011	-0.15266202267E-03	-1.514(42) 10^{-4}
221	R3(1,1E)	002000 000011	0.56490411197E-04	5.68(41) 10^{-5}
222	R3(3,3A$_1$)	002000 000011	0.99561331956E-04	9.90(24) 10^{-5}
223	R3(3,0A$_2$)	002000 000011	0.22899032984E-04	2.09(33) 10^{-5}
224	R3(3,3A$_2$)	002000 000011	0.10709405518E-03	1.078(15) 10^{-4}
225	R3(3,1E)	002000 000011	-0.69441263659E-04	-6.96(39) 10^{-5}
226	R0(0,0A$_1$)	001010 001010	-0.36578658037E+01	-3.65780(37)
227	R1(1,0A$_2$)	001010 001010	0.19589200393E-01	1.950(16) 10^{-2}
228	R2(2,1E)	001010 001010	0.13735578480E-01	1.370(36) 10^{-2}
229	R2(2,2E)	001010 001010	0.14246879162E-01	1.4255(98) 10^{-2}
230	R3(3,0A$_2$)	001010 001010	-0.38819203106E-04	-3.85(11) 10^{-5}
231	R4(2,0A$_1$)	001010 001010	0.43322520838E-05	4.326(57) 10^{-6}
232	R4(2,1E)	001010 001010	0.43574710042E-05	4.29(22) 10^{-6}
233	R4(2,2E)	001010 001010	-0.60124841963E-05	-6.00(15) 10^{-6}
234	R4(4,0A$_1$)	001010 001010	0.28061935894E-05	2.802(45) 10^{-6}
235	R4(4,3A$_1$)	001010 001010	0.14041618278E-05	1.36(18) 10^{-6}
236	R4(4,1E)	001010 001010	-0.54937435648E-05	-5.49(14) 10^{-6}
237	R4(4,2E)	001010 001010	0.70019152009E-05	7.01(13) 10^{-6}
238	R4(4,4E)	001010 001010	0.32733648069E-05	3.263(80) 10^{-6}
239	R0(0,0A$_1$)	001001 001001	-0.34426075531E+01	-3.4422(45)
240	R1(1,0A$_2$)	001001 001001	-0.21783877884E-01	-2.179(11) 10^{-2}
241	R2(0,0A$_1$)	001001 001001	0.35660254627E-02	3.559(34) 10^{-3}
242	R2(2,2E)	001001 001001	0.12334695141E-02	1.233(17) 10^{-3}
243	R3(3,0A$_2$)	001001 001001	0.25921155623E-04	2.567(30) 10^{-5}
244	R3(3,3A$_2$)	001001 001001	-0.20584073671E-03	-2.044(41) 10^{-4}
245	R4(0,0A$_1$)	001001 001001	0.57736930050E-05	5.69(14) 10^{-6}
246	R4(2,1E)	001001 001001	0.46423411893E-05	4.62(23) 10^{-6}
247	R4(2,2E)	001001 001001	0.80086749315E-05	7.951(81) 10^{-6}

Appendix - Effective Hamiltonian Terms for the Nonad of CH_3D (Continued)

	Tensorial Nomenclature		Parameter value	
	Rotational	Vibrational	Computer Input	Rounded (St. Dev.)
248	R4(4,0A_1)	001001 001001	0.55836382761E-06	5.56(16) 10^{-7}
249	R4(4,1E)	001001 001001	0.51552960223E-05	5.09(13) 10^{-6}
250	R4(4,2E)	001001 001001	-0.47661425489E-05	-4.788(96) 10^{-6}
251	R4(4,4E)	001001 001001	0.33602249225E-05	3.333(48) 10^{-6}
252	R1(1,0A_2)	001010 000100	-0.30548311556E+00	-3.024(90) 10^{-1}
253	R1(1,1E)	001010 000100	-0.15335953171E+01	-1.540(14)
254	R2(2,0A_1)	001010 000100	-0.62502170756E-02	-6.28(39) 10^{-3}
255	R2(2,2E)	001010 000100	0.80800103518E-02	8.16(56) 10^{-3}
256	R3(1,0A_2)	001010 000100	-0.37349807391E-03	-3.73(10) 10^{-4}
257	R3(1,1E)	001010 000100	-0.27915167060E-03	-2.82(14) 10^{-4}
258	R3(3,3A_1)	001010 000100	0.11927897840E-03	1.188(67) 10^{-4}
259	R3(3,1E)	001010 000100	0.19716140564E-03	2.01(17) 10^{-4}
260	R3(3,2E)	001010 000100	-0.24272780227E-03	-2.43(27) 10^{-4}
261	R4(0,0A_1)	001010 000100	-0.32547514772E-05	-3.25(15) 10^{-6}
262	R4(2,1E)	001010 000100	-0.65180990624E-05	-6.48(42) 10^{-6}
263	R4(2,2E)	001010 000100	0.77461795584E-05	7.68(53) 10^{-6}
264	R4(4,0A_1)	001010 000100	0.19120185795E-05	1.90(17) 10^{-6}
265	R4(4,3A_1)	001010 000100	-0.29344059493E-05	-2.84(29) 10^{-6}
266	R4(4,3A_2)	001010 000100	-0.75868306933E-05	-7.54(27) 10^{-6}
267	R4(4,1E)	001010 000100	0.48499003957E-05	4.84(26) 10^{-6}
268	R4(4,4E)	001010 000100	-0.70246108062E-05	-6.96(32) 10^{-6}
269	R2(2,1E)	001010 000020	0.49421768649E-02	4.92(18) 10^{-3}
270	R2(2,2E)	001010 000020	-0.13902215823E-01	-1.375(31) 10^{-2}
271	R3(1,1E)	001010 000020	-0.22423780479E-03	-2.229(56) 10^{-4}
272	R1(1,0A_2)	001010 000020	-0.23027390307E+00	-2.292(68) 10^{-1}
273	R2(0,0A_1)	001010 000020	-0.20390606926E-01	-2.019(22) 10^{-2}
274	R2(2,2E)	001010 000020	-0.19649936329E-01	-1.951(25) 10^{-2}
275	R3(1,0A_2)	001010 000020	-0.13302212915E-03	-1.323(63) 10^{-4}
276	R3(1,1E)	001010 000020	0.21544841604E-04	2.27(45) 10^{-5}
277	R3(3,3A_1)	001010 000020	0.13623715251E-03	1.354(31) 10^{-4}
278	R3(3,0A_2)	001010 000020	-0.18291876501E-03	-1.806(45) 10^{-4}
279	R3(3,2E)	001010 000020	-0.11700071639E-03	-1.178(59) 10^{-4}
280	R0(0,0A_1)	001010 000011	0.65666661594E+00	6.48(56) 10^{-1}
281	R1(1,0A_2)	001010 000011	0.15026647517E+00	1.475(56) 10^{-1}
282	R1(1,1E)	001010 000011	0.76596964458E+00	7.626(39) 10^{-1}
283	R2(2,0A_1)	001010 000011	-0.36592199725E-02	-3.70(16) 10^{-3}
284	R2(2,1E)	001010 000011	-0.54024510580E-02	-5.51(28) 10^{-3}
285	R2(2,1E)	001010 000011	0.11179523230E-01	1.111(20) 10^{-2}
286	R2(2,1E)	001010 000011	0.19457649285E-01	1.939(22) 10^{-2}
287	R2(2,2E)	001010 000011	-0.19543150701E-02	-1.976(87) 10^{-3}
288	R2(2,2E)	001010 000011	-0.47751673375E-02	-4.87(19) 10^{-3}
289	R3(1,1E)	001010 000011	0.23857927614E-03	2.371(39) 10^{-4}
290	R3(1,1E)	001010 000011	0.59658046375E-04	5.98(52) 10^{-5}
291	R3(3,3A_1)	001010 000011	0.14076068811E-03	1.393(20) 10^{-4}
292	R3(3,1E)	001010 000011	0.74103323280E-04	7.56(30) 10^{-5}
293	R3(3,1E)	001010 000011	-0.16998106152E-03	-1.727(49) 10^{-4}
294	R3(3,1E)	001010 000011	0.11705513864E-03	1.169(72) 10^{-4}
295	R3(3,2E)	001010 000011	0.92670774705E-04	9.08(45) 10^{-5}
296	R3(3,2E)	001010 000011	-0.19221390549E-03	-1.937(45) 10^{-4}
297	R0(0,0A_1)	001001 000011	0.41304667871E+01	4.13(12)

Appendix - Effective Hamiltonian Terms for the Nonad of CH_3D (Continued)

	Tensorial Nomenclature		Parameter value	
	Rotational	Vibrational	Computer Input	Rounded (St. Dev.)
298	R2(0,0A_1)	001001 000011	-0.61815546110E-02	-6.07(15) 10^{-3}
299	R2(2,0A_1)	001001 000011	0.97644210651E-02	9.74(21) 10^{-3}
300	R2(2,1E)	001001 000011	0.50406833906E-02	5.08(11) 10^{-3}
301	R2(2,2E)	001001 000011	0.15248265564E-01	1.522(13) 10^{-2}
302	R2(2,2E)	001001 000011	-0.42675836768E-02	-4.25(19) 10^{-3}
303	R2(2,2E)	001001 000011	-0.48639541206E-02	-4.81(13) 10^{-3}
304	R3(1,0A_2)	001001 000011	-0.11376291791E-03	-1.130(34) 10^{-4}
305	R3(1,1E)	001001 000011	0.60114496969E-04	6.00(18) 10^{-5}
306	R3(1,1E)	001001 000011	0.19621841433E-03	1.943(31) 10^{-4}
307	R3(3,3A_1)	001001 000011	-0.59958320306E-04	-5.92(13) 10^{-5}
308	R3(3,0A_2)	001001 000011	0.10422578557E-03	1.033(29) 10^{-4}
309	R3(3,3A_2)	001001 000011	-0.66655675924E-04	-6.52(12) 10^{-5}
310	R3(3,1E)	001001 000011	-0.11605545022E-03	-1.160(20) 10^{-4}
311	R3(3,1E)	001001 000011	-0.18632215161E-03	-1.855(23) 10^{-4}
312	R3(3,1E)	001001 000011	-0.15104815101E-03	-1.505(34) 10^{-4}
313	R3(3,2E)	001001 000011	0.51245378462E-04	5.07(31) 10^{-5}
314	R3(3,2E)	001001 000011	0.87091364580E-04	9.06(46) 10^{-5}
315	R2(2,1E)	001001 000002	-0.37999162617E-02	-3.80(13) 10^{-3}
316	R2(2,2E)	001001 000002	-0.23714991808E-02	-2.40(10) 10^{-3}
317	R3(1,1E)	001001 000002	0.66311371566E-04	6.58(26) 10^{-5}
318	R3(3,1E)	001001 000002	0.10880734017E-03	1.106(31) 10^{-4}
319	R1(1,1E)	001001 000002	0.14056237729E+00	1.4049(25) 10^{-1}
320	R2(0,0A_1)	001001 000002	-0.88435138753E-02	-8.834(60) 10^{-3}
321	R2(2,0A_1)	001001 000002	0.94587536351E-02	9.445(84) 10^{-3}
322	R2(2,1E)	001001 000002	0.20056954883E-02	1.97(12) 10^{-3}
323	R2(2,2E)	001001 000002	-0.48817088750E-02	-4.854(81) 10^{-3}
324	R3(1,1E)	001001 000002	-0.59098276369E-04	-5.89(13) 10^{-5}
325	R3(3,3A_1)	001001 000002	0.40386434334E-04	4.04(10) 10^{-5}
326	R3(3,0A_2)	001001 000002	0.93512121354E-04	9.41(39) 10^{-5}
327	R3(3,1E)	001001 000002	0.39145862588E-04	3.88(15) 10^{-5}
328	R0(0,0A_1)	000100 000100	0.30167096477E+04	3016.70965(15)
329	R1(1,0A_2)	000100 000100	-0.54230593454E+00	-5.42271(78) 10^{-1}
330	R2(0,0A_1)	000100 000100	-0.25948407371E-01	-2.5959(65) 10^{-2}
331	R2(2,0A_1)	000100 000100	-0.48029069523E-02	-4.779(32) 10^{-3}
332	R2(2,1E)	000100 000100	-0.84464218623E-02	-8.45(55) 10^{-3}
333	R2(2,2E)	000100 000100	-0.16171984687E-02	-1.620(27) 10^{-3}
334	R3(1,0A_2)	000100 000100	-0.26479312586E-04	-2.68(19) 10^{-5}
335	R3(3,3A_2)	000100 000100	-0.26110134376E-04	-2.64(19) 10^{-5}
336	R4(0,0A_1)	000100 000100	0.21280607424E-05	2.11(17) 10^{-6}
337	R4(2,1E)	000100 000100	0.37814599755E-05	3.84(37) 10^{-6}
338	R4(4,0A_1)	000100 000100	-0.11044339845E-05	-1.109(43) 10^{-6}
339	R4(4,3A_1)	000100 000100	0.19808491359E-04	1.974(58) 10^{-5}
340	R4(4,2E)	000100 000100	-0.38658649317E-05	-3.839(98) 10^{-6}
341	R5(3,0A_2)	000100 000100	0.22493765165E-07	2.251(90) 10^{-8}
342	R5(3,3A_2)	000100 000100	-0.23869315131E-07	-2.36(17) 10^{-8}
343	R6(0,0A_1)	000100 000100	-0.15108285616E-07	-1.505(24) 10^{-8}
344	R6(4,3A_1)	000100 000100	0.33365414257E-07	3.319(61) 10^{-8}
345	R6(6,3A_1)	000100 000100	0.29175342775E-08	2.97(28) 10^{-9}
346	R6(6,1E)	000100 000100	-0.36646130798E-08	-3.65(12) 10^{-9}
347	R6(6,4E)	000100 000100	-0.24847121339E-08	-2.474(96) 10^{-9}

Appendix - Effective Hamiltonian Terms for the Nonad of CH_3D (Continued)

	Tensorial Nomenclature		Parameter value	
	Rotational	Vibrational	Computer Input	Rounded (St. Dev.)
348	R6(6,5E)	000100 000100	0.60002940449E-08	6.00(26) 10^{-9}
349	R2(2,1E)	000100 000020	0.17512297282E-01	1.747(55) 10^{-2}
350	R2(2,2E)	000100 000020	0.46264484974E-02	4.73(37) 10^{-3}
351	R3(1,1E)	000100 000020	-0.21877866447E-03	-2.166(93) 10^{-4}
352	R3(3,1E)	000100 000020	-0.16698445607E-03	-1.661(88) 10^{-4}
353	R3(3,2E)	000100 000020	-0.52912560253E-03	-5.252(93) 10^{-4}
354	R4(2,1E)	000100 000020	0.73767293682E-05	7.22(59) 10^{-6}
355	R4(4,2E)	000100 000020	-0.13865663536E-04	-1.383(16) 10^{-5}
356	R4(4,4E)	000100 000020	0.28293464073E-05	2.78(14) 10^{-6}
357	R1(1,0A_2)	000100 000020	-0.83025721249E+00	-8.2953(93) 10^{-1}
358	R2(2,0A_1)	000100 000020	-0.21631294786E-02	-2.12(10) 10^{-3}
359	R2(2,1E)	000100 000020	0.14446465246E-01	1.442(30) 10^{-2}
360	R2(2,2E)	000100 000020	-0.73815740318E-02	-7.31(21) 10^{-3}
361	R3(3,3A_1)	000100 000020	0.15451006337E-03	1.521(61) 10^{-4}
362	R3(3,0A_2)	000100 000020	-0.64847504363E-04	-6.38(33) 10^{-5}
363	R3(3,1E)	000100 000020	-0.13381734079E-03	-1.34(10) 10^{-4}
364	R3(3,2E)	000100 000020	-0.13980335798E-03	-1.376(84) 10^{-4}
365	R4(2,0A_1)	000100 000020	0.14836525431E-05	1.465(95) 10^{-6}
366	R4(2,2E)	000100 000020	-0.44615179768E-05	-4.37(19) 10^{-6}
367	R4(4,0A_1)	000100 000020	-0.99220250570E-06	-1.003(82) 10^{-6}
368	R4(4,3A_1)	000100 000020	0.54067360604E-05	5.36(24) 10^{-6}
369	R4(4,3A_2)	000100 000020	0.36391381435E-05	3.64(22) 10^{-6}
370	R4(4,1E)	000100 000020	-0.60616491846E-05	-6.08(14) 10^{-6}
371	R4(4,4E)	000100 000020	0.25872365355E-05	2.568(90) 10^{-6}
372	R0(0,0A_1)	000020 000020	-0.33694391997E+02	-33.689(12)
373	R2(0,0A_1)	000020 000020	-0.22846312732E-01	-2.275(22) 10^{-2}
374	R2(2,0A_1)	000020 000020	0.66448415069E-02	6.613(78) 10^{-3}
375	R4(0,0A_1)	000020 000020	0.11972746922E-04	1.185(47) 10^{-5}
376	R4(2,0A_1)	000020 000020	0.25835443166E-05	2.586(73) 10^{-6}
377	R1(1,1E)	000020 000020	-0.73806630214E-01	-7.42(31) 10^{-2}
378	R2(2,1E)	000020 000020	-0.62837994920E-02	-6.25(12) 10^{-3}
379	R2(2,2E)	000020 000020	0.35559728592E-02	3.52(10) 10^{-3}
380	R3(3,1E)	000020 000020	0.10747842171E-03	1.075(35) 10^{-4}
381	R3(3,2E)	000020 000020	-0.12869005077E-03	-1.281(68) 10^{-4}
382	R0(0,0A_1)	000020 000020	-0.55770095420E+01	-5.57702(18)
383	R1(1,0A_2)	000020 000020	0.27531980024E+00	2.75326(32) 10^{-1}
384	R2(0,0A_1)	000020 000020	-0.18082389155E-02	-1.819(22) 10^{-3}
385	R2(2,1E)	000020 000020	0.57209719282E-01	5.681(58) 10^{-2}
386	R3(1,0A_2)	000020 000020	-0.11235160400E-03	-1.102(34) 10^{-4}
387	R3(3,0A_2)	000020 000020	-0.70364732344E-04	-6.92(25) 10^{-5}
388	R3(3,3A_2)	000020 000020	0.32402607937E-03	3.237(47) 10^{-4}
389	R4(0,0A_1)	000020 000020	-0.17183068273E-04	-1.699(29) 10^{-5}
390	R4(2,0A_1)	000020 000020	-0.29110936288E-05	-2.908(70) 10^{-6}
391	R4(2,1E)	000020 000020	-0.33536429065E-05	-3.22(28) 10^{-6}
392	R4(2,2E)	000020 000020	-0.11329757472E-05	-1.10(11) 10^{-6}
393	R4(4,1E)	000020 000020	0.75573123164E-05	7.46(23) 10^{-6}
394	R4(4,2E)	000020 000020	0.41643186340E-05	4.13(15) 10^{-6}
395	R4(4,4E)	000020 000020	-0.25618899001E-05	-2.56(18) 10^{-6}
396	R0(0,0A_1)	000011 000011	-0.93046432438E+01	-9.3066(52)
397	R0(0,0A_1)	000011 000011	0.10175843441E+02	10.1743(64)

Appendix - Effective Hamiltonian Terms for the Nonad of CH_3D (Continued)

	Tensorial Nomenclature		Parameter value	
	Rotational	Vibrational	Computer Input	Rounded (St. Dev.)
398	R0(0,0A_1)	000011 000011	-0.18059056398E+01	-1.8083(69)
399	R1(1,0A_2)	000011 000011	-0.22917531834E-01	-2.288(20) 10^{-2}
400	R1(1,0A_2)	000011 000011	-0.36249871679E-01	-3.632(27) 10^{-2}
401	R1(1,1E)	000011 000011	-0.12370297666E+00	-1.229(38) 10^{-1}
402	R2(0,0A_1)	000011 000011	-0.90726017544E-02	-9.095(29) 10^{-3}
403	R2(0,0A_1)	000011 000011	0.53431912971E-02	5.346(65) 10^{-3}
404	R2(0,0A_1)	000011 000011	0.25804269237E-01	2.552(27) 10^{-2}
405	R2(2,0A_1)	000011 000011	0.23989975318E-02	2.398(13) 10^{-3}
406	R2(2,0A_1)	000011 000011	-0.23864315507E-02	-2.387(18) 10^{-3}
407	R2(2,0A_1)	000011 000011	0.98853101479E-02	9.75(17) 10^{-3}
408	R2(2,1E)	000011 000011	0.56108851919E-02	5.43(46) 10^{-3}
409	R2(2,1E)	000011 000011	-0.12753824714E-01	-1.266(23) 10^{-2}
410	R2(2,2E)	000011 000011	0.60188830139E-02	6.013(22) 10^{-3}
411	R2(2,2E)	000011 000011	-0.22438436329E-03	-2.16(26) 10^{-4}
412	R3(1,0A_2)	000011 000011	-0.94735870798E-04	-9.44(17) 10^{-5}
413	R3(1,0A_2)	000011 000011	0.12613568903E-03	1.261(18) 10^{-4}
414	R3(1,1E)	000011 000011	0.15182488233E-03	1.493(52) 10^{-4}
415	R3(1,1E)	000011 000011	0.52856868825E-04	5.28(42) 10^{-5}
416	R3(3,0A_2)	000011 000011	-0.69133694839E-04	-6.95(14) 10^{-5}
417	R3(3,0A_2)	000011 000011	0.94079235528E-04	9.44(16) 10^{-5}
418	R3(3,3A_2)	000011 000011	0.36889559617E-04	3.78(35) 10^{-5}
419	R3(3,1E)	000011 000011	0.76166162258E-04	7.38(29) 10^{-5}
420	R0(0,0A_1)	000002 000002	-0.59314134376E+01	-5.93139(10)
421	R2(0,0A_1)	000002 000002	0.77229437182E-02	7.719(16) 10^{-3}
422	R2(2,0A_1)	000002 000002	-0.40201134794E-02	-4.017(12) 10^{-3}
423	R4(4,0A_1)	000002 000002	-0.22121138651E-06	-2.24(26) 10^{-7}
424	R4(4,3A_1)	000002 000002	-0.67209796086E-06	-7.07(44) 10^{-7}
425	R1(1,1E)	000002 000002	-0.33612540790E-01	-3.33(15) 10^{-2}
426	R2(2,1E)	000002 000002	-0.73894051400E-02	-7.32(40) 10^{-3}
427	R2(2,2E)	000002 000002	-0.58916771280E-02	-5.890(11) 10^{-3}
428	R3(1,1E)	000002 000002	-0.69218193397E-04	-7.05(31) 10^{-5}
429	R3(3,1E)	000002 000002	0.49260407753E-04	5.23(50) 10^{-5}
430	R0(0,0A_1)	000002 000002	0.15412294814E+01	1.54122(11)
431	R1(1,0A_2)	000002 000002	0.44161847332E-01	4.4167(15) 10^{-2}
432	R2(2,0A_1)	000002 000002	-0.90760027291E-03	-9.058(83) 10^{-4}
433	R2(2,2E)	000002 000002	0.10954099576E-02	1.091(11) 10^{-3}
434	R3(1,0A_2)	000002 000002	0.23761095296E-04	2.37(10) 10^{-5}
435	R3(3,0A_2)	000002 000002	-0.13812937301E-04	-1.375(94) 10^{-5}
436	R4(0,0A_1)	000002 000002	0.28425219592E-05	2.846(85) 10^{-6}
437	R4(2,1E)	000002 000002	-0.69274807443E-05	-6.90(21) 10^{-6}
438	R4(2,2E)	000002 000002	-0.21327258198E-05	-2.31(25) 10^{-6}
439	R4(4,0A_1)	000002 000002	-0.66194760406E-06	-6.65(17) 10^{-7}
440	R4(4,3A_1)	000002 000002	-0.29402472432E-05	-2.925(49) 10^{-6}
441	R4(4,2E)	000002 000002	0.37521435164E-05	4.03(38) 10^{-6}

For clarity, only a simplified nomenclature is reported here. The complete unambiguous tensorial nomenclature is available from the electronic file at http://www.u-bourgogne.fr/LPUB/MIRS.html

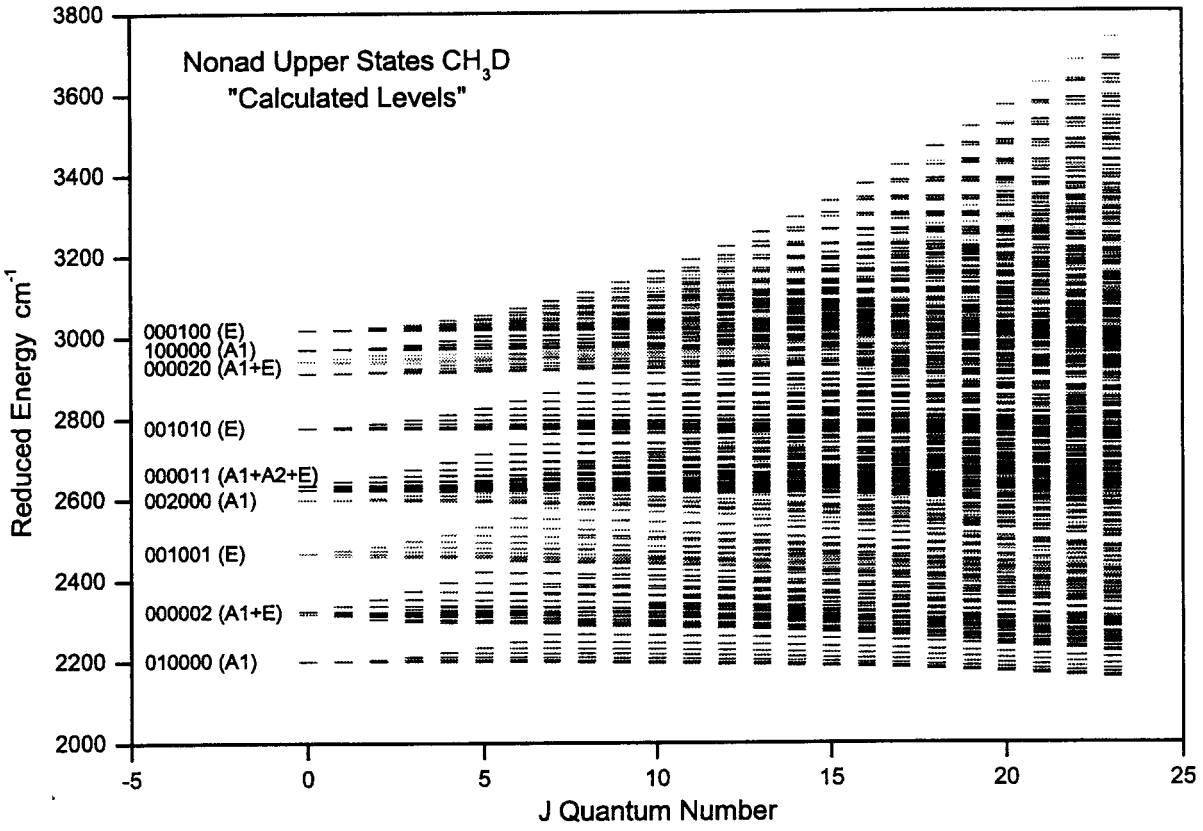

Figure 1. (Top) Reduced upper state energies versus upper state J for the nine bands (nonad) of CH_3D between 3 and 5 μm. Upper pannel: calculated levels

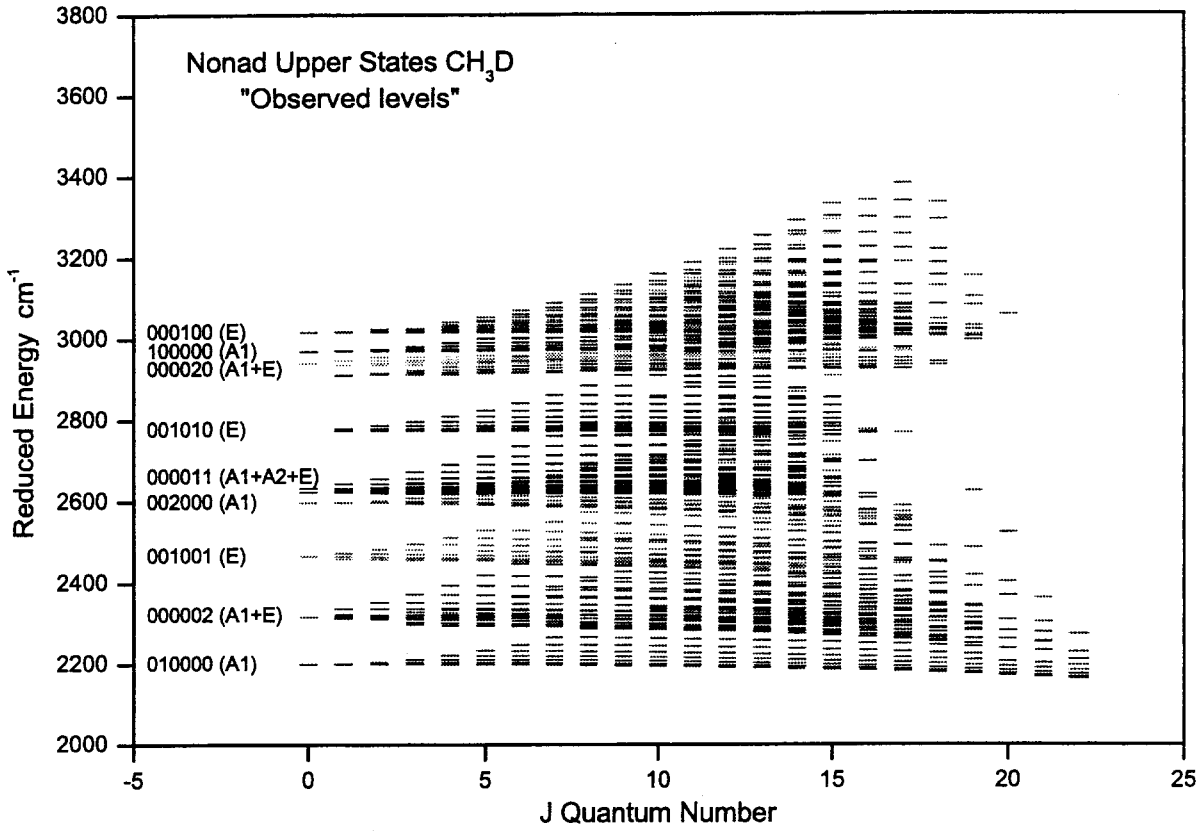

Figure 1. (Bottom) Reduced upper state energies versus upper state J for the nine bands (nonad) of CH_3D between 3 and 5 μm. Lower pannel: assigned and fitted levels

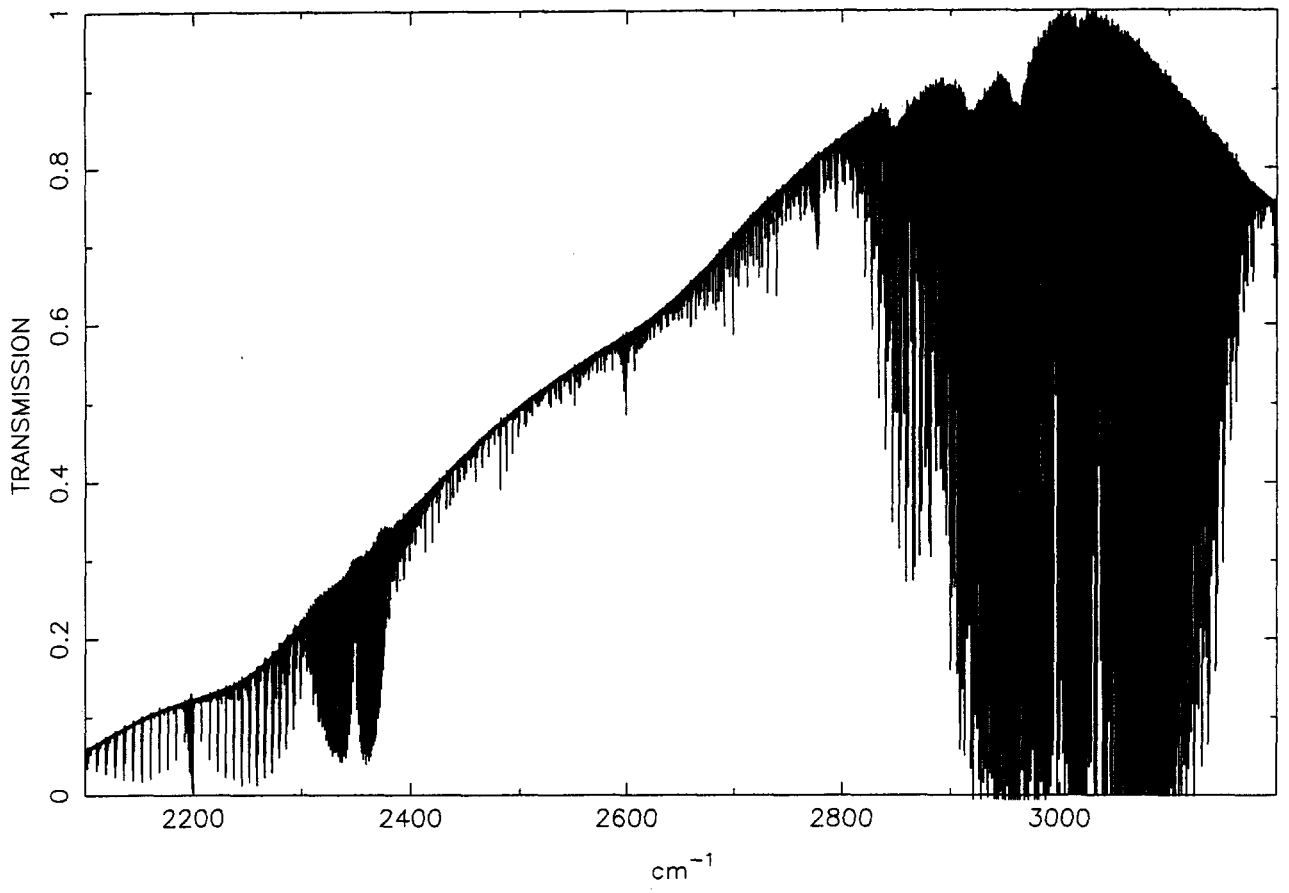

Figure 2a. The unapodized spectrum of CH_3D observed with the Fourier transform spectrometer located at Kitt Peak National Observatory. The resolution is 0.012 cm^{-1}. The gas pressure is 15.5 Torr at 293.4 K of an enriched sample containing 98% CH_3D. The optical path is 10 cm. The strongest band in the region is ν_4 near 3017 cm^{-1}. The band near 2350 cm^{-1} arises from residual CO_2.

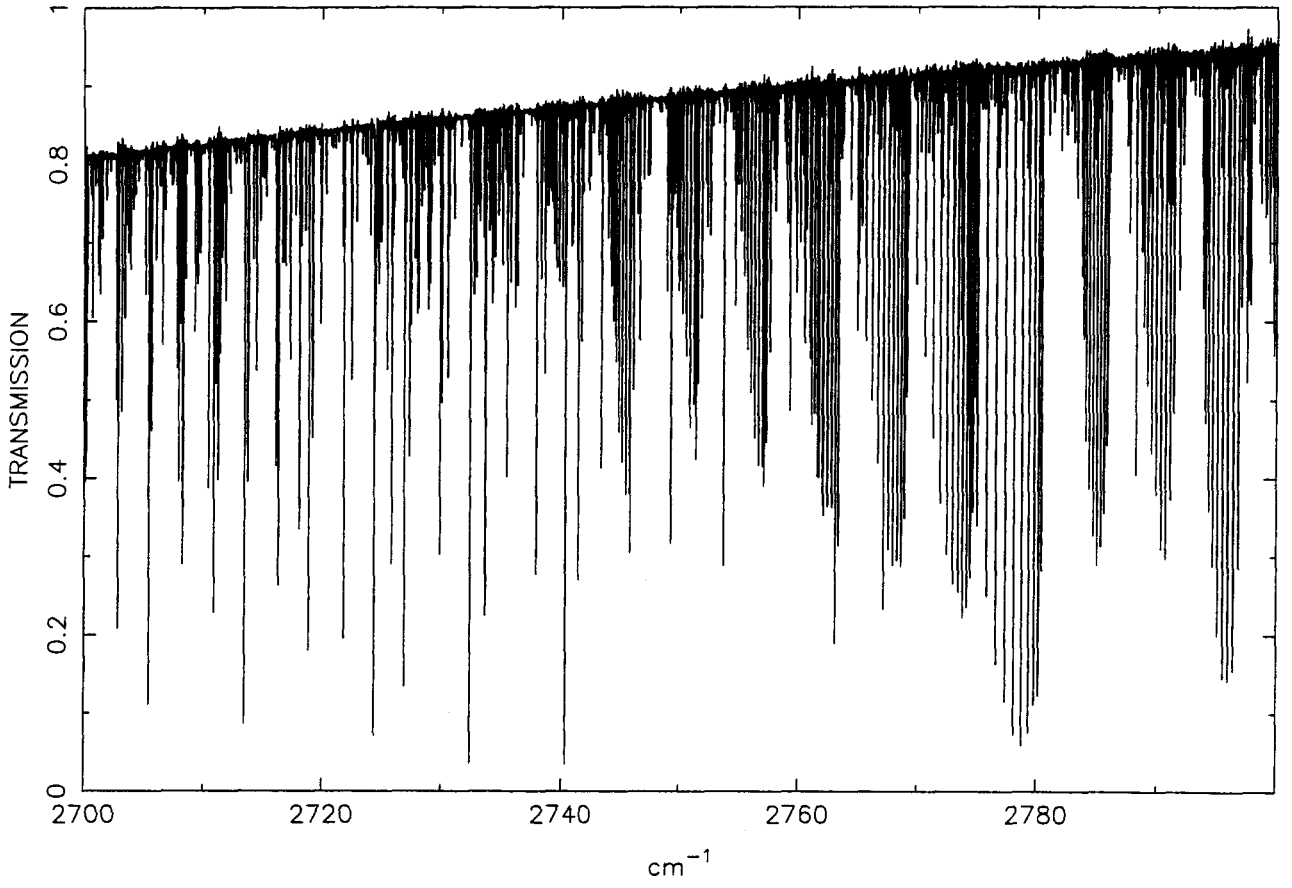

Figure 2b. The Spectrum of CH_3D observed with the Fourier transform spectrometer located at Kitt Peak Notional Observatory. The resolution is 0.012 cm^{-1}. The gas pressure is 20 Torr at 295 K, and the path is 1.5 m. The strong Q branches near 2780 cm^{-1} belong to $\nu_3 + \nu_5(E)$.

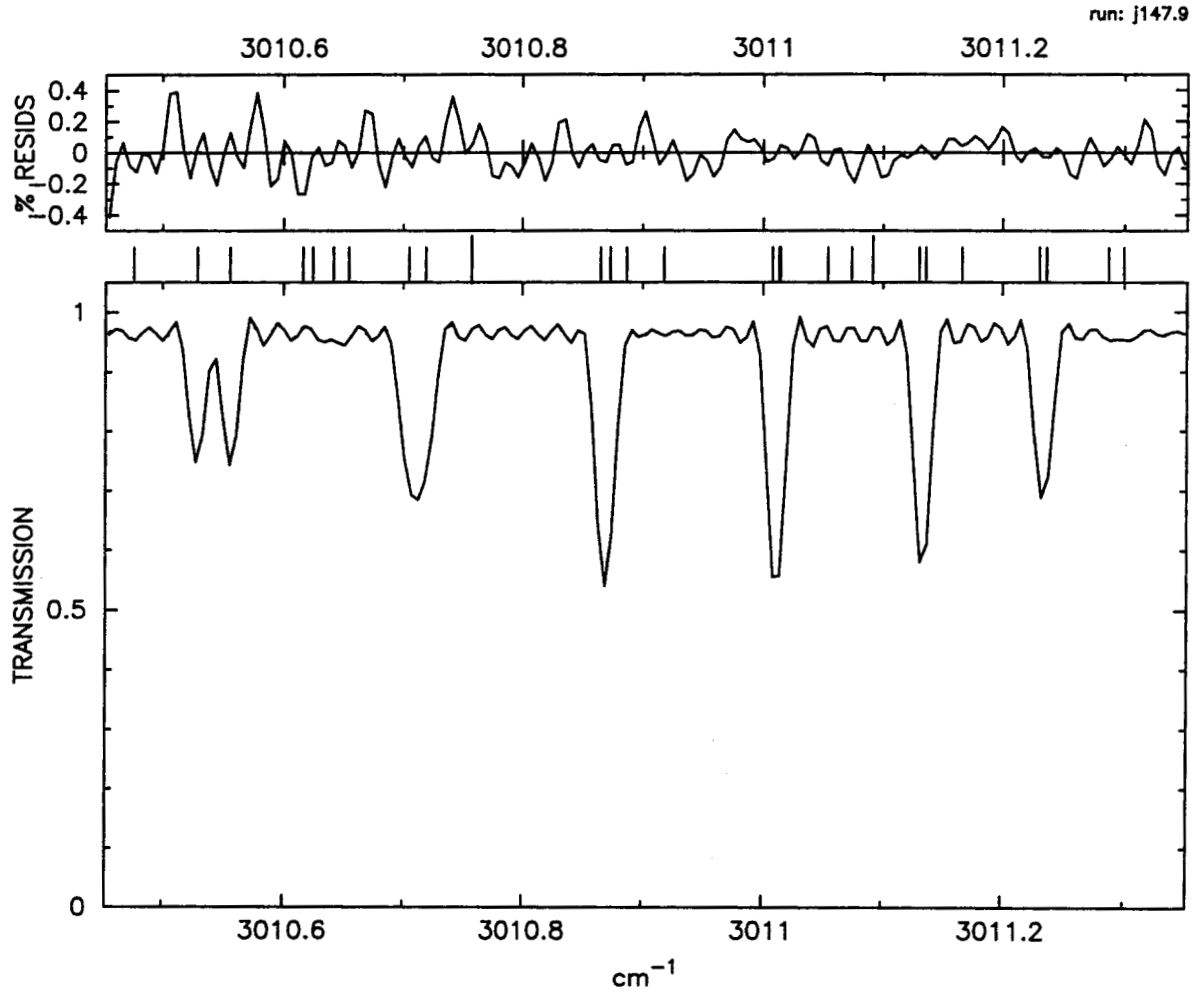

Figure 3. Retrieval of positions and intensities by least squares curve fitting in the Q branch region of ν_4. The observed and synthetic spectra are overplotted in the lower panel and the residual differences are shown in the upper panel. The gas pressure is 4.98 Torr at 296.1 K, and the optical path is 0.0205 cm.

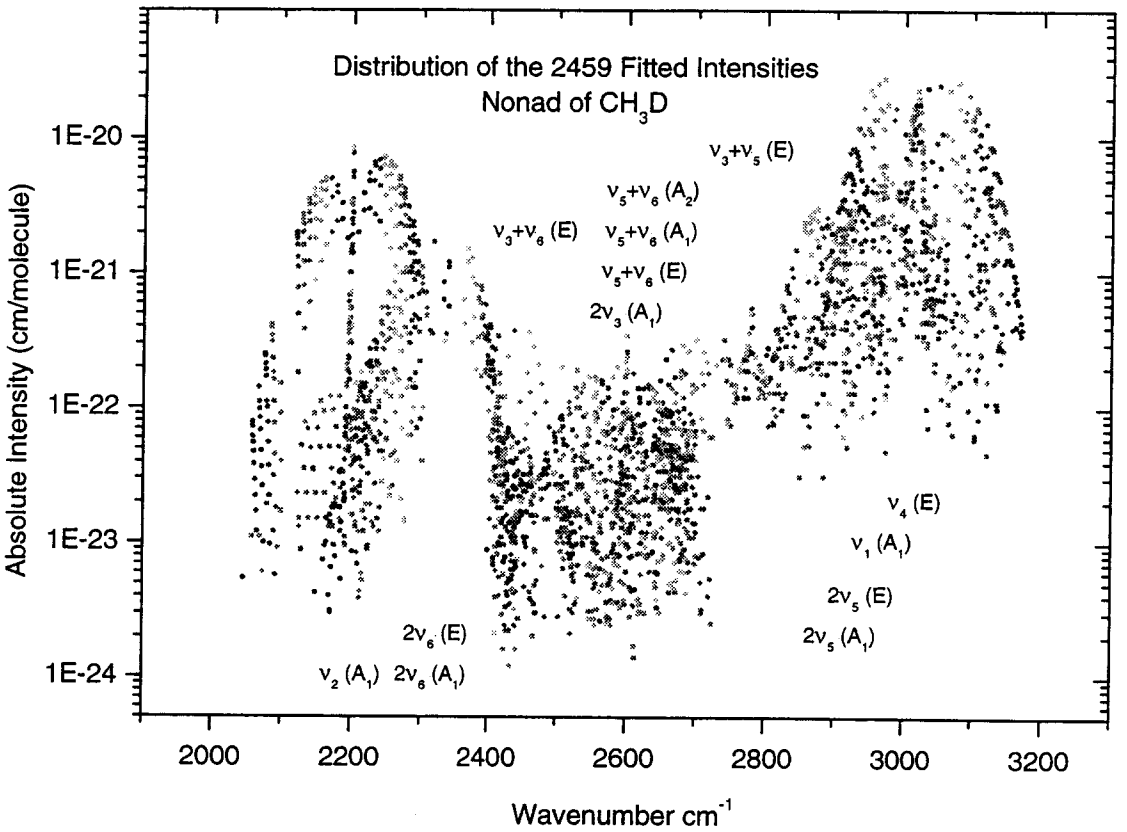

Figure 4. Distribution of measured line intensities in the nonad. The observed intensities are plotted as a function of the line positions. Values in cm^{-2} atm^{-1} at 296 K have been multiplied by 4.033×10^{-20} to convert to the intensity units of HITRAN (cm/molecule).

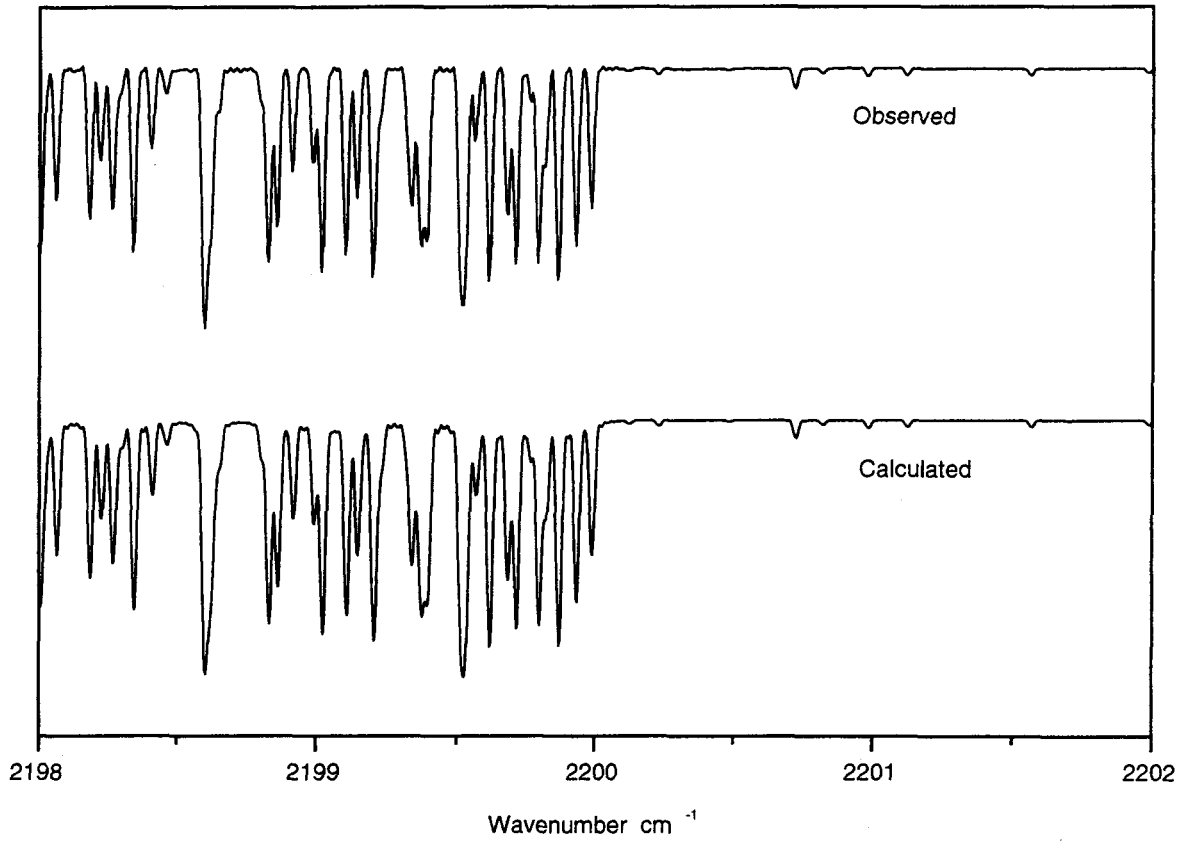

Figure 5a. Examples of calculated (lower trace) and observed spectra of CH_3D. $P(J = 14)$ branch of ν_2. The gas pressure is 0.721 Torr at 291 K, and the path is 2.4 m.

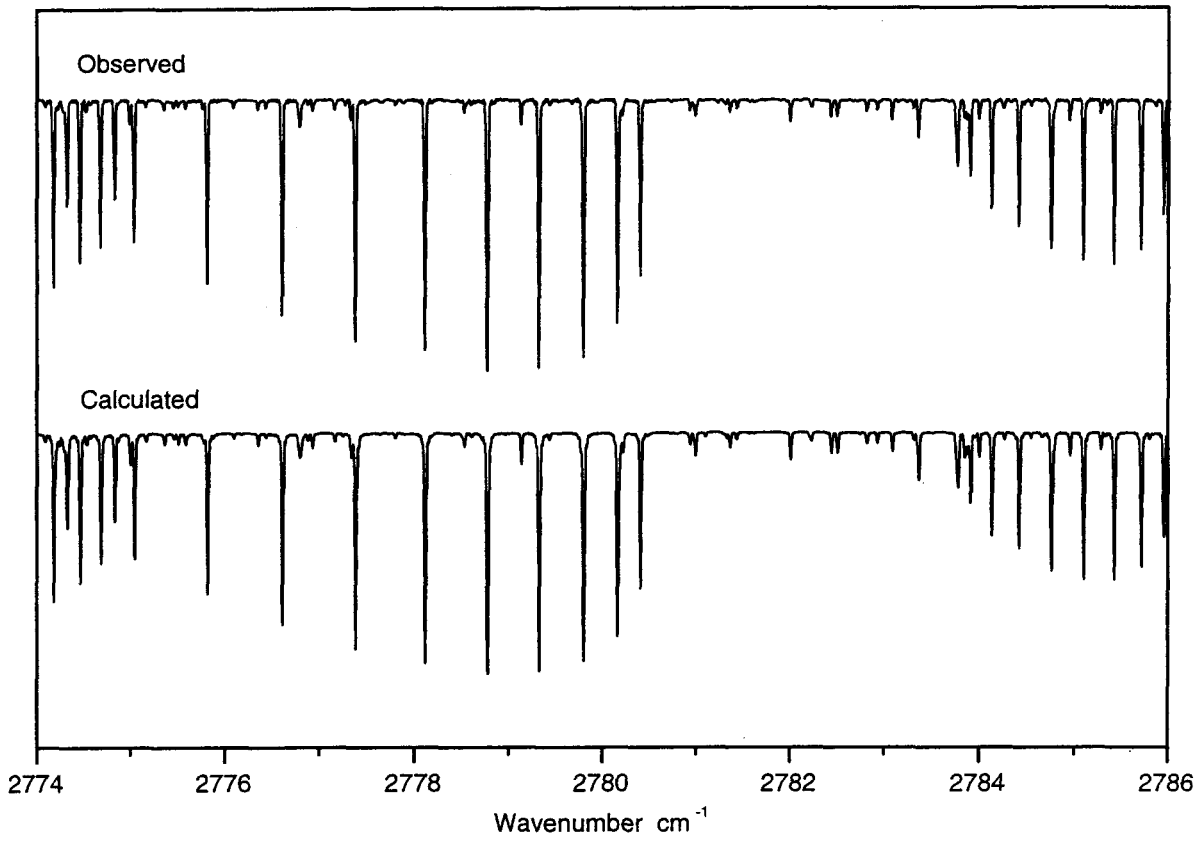

Figure 5b. Examples of calculated (lower trace) and observed spectra of CH_3D. $RQ(K=0)$ of $\nu_3+\nu_5$ (E) at 2780 cm^{-1} The gas pressure is 4.88 Torr at 291 K, and the path is 2.4 m.

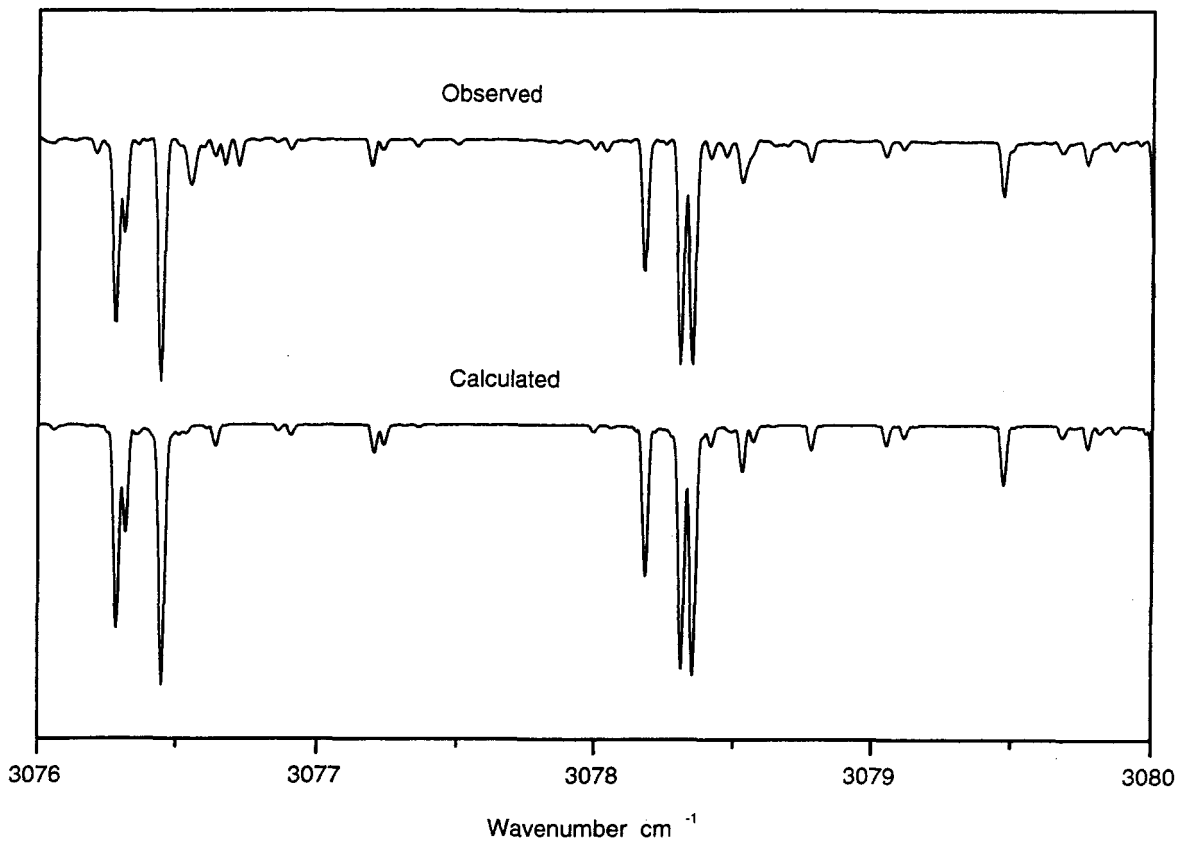

Figure 5c. Examples of calculated (lower trace) and observed spectra of CH_3D. R branch of ν_4 at 3078 cm^{-1} The gas pressure is 0.721 Torr at 291 K, and the path is 2.4 m. Extra lines in the upper trace arise from residual CH_4.